62 64848 387

CONFIDENTIAL

Copy
RM E58G10a

N63-12517
code-1

UNCLASSIFIED

NACA RM E58G10a

RESEARCH MEMORANDUM

OFF-DESIGN PERFORMANCE OF DIVERGENT EJECTORS

By Milton A. Beheim

Lewis Flight Propulsion Laboratory
Cleveland, Ohio

OTS PRICE
XEROX $ 6.60 ph
MICROFILM $ 2.00 mf

CLASSIFICATION CHANGED TO
UNCLASSIFIED - AUTHORITY:
NASA - EFFECTIVE DATE
SEPTEMBER 14, 1962

CLASSIFIED DOCUMENT

This material contains information affecting the National Defense of the United States within the meaning of the espionage laws, Title 18, U.S.C., Secs. 793 and 794, the transmission or revelation of which in any manner to an unauthorized person is prohibited by law.

NATIONAL ADVISORY COMMITTEE
FOR AERONAUTICS

WASHINGTON

September 30, 1958

CONFIDENTIAL

NATIONAL ADVISORY COMMITTEE FOR AERONAUTICS

RESEARCH MEMORANDUM

OFF-DESIGN PERFORMANCE OF DIVERGENT EJECTORS *

By Milton A. Beheim

SUMMARY

The off-design performance of fixed- and of variable-geometry divergent ejectors was investigated. The ejectors, which were designed for turbojet operation at Mach 3, were investigated in the Mach number range 0.8 to 2. The performance of a fixed-geometry ejector with high secondary-flow rates was competitive with that of more complex variable-geometry ejectors. Variable-geometry ejectors with compromises to reduce mechanical complexity produced performance reasonably close to that of an ideal variable ejector.

INTRODUCTION

Simple fixed-geometry divergent ejectors designed for good performance at high flight speeds (e.g., Mach 3) suffer large performance losses at low speeds. This loss results from jet overexpansion, which depends on the geometry and the jet and stream interaction. Analyses have shown that the performance of such an ejector can be so poor at low speeds that an airplane would not be able to accelerate to the high design speed. In other cases where sufficient thrust was available during acceleration, excessive fuel consumption occurred.

The following techniques of solving the problem are considered in this investigation: (1) Compromise the design performance to improve off-design performance; (2) employ variable geometry; (3) employ large amounts of secondary airflow to fill in the excess area of the exit. These schemes were investigated in the NACA Lewis 8- by 6-foot tunnel in the Mach number range 0.8 to 2.

SYMBOLS

C_D boattail drag coefficient based on maximum cross-sectional area

D boattail plus base drag

*Title, Unclassified.

d_B base diameter

d_e exit diameter

d_m maximum forebody diameter

d_p primary-nozzle diameter

d_r spoiler diameter

d_s secondary-nozzle diameter

F ejector gross thrust

F_i gross thrust of ideal completely expanded primary flow

l axial distance from primary-nozzle exit to ejector exit

M Mach number

m_b bypass mass-flow rate

m_s secondary mass-flow rate

m_0 maximum capture mass-flow rate of inlet

P_p primary total pressure

P_s secondary total pressure

P_0 free-stream total pressure (upstream of model)

P_l local Pitot pressure

p_B base static pressure

p_{bt} boattail static pressure

p_e exit-plane static pressure

p_0 free-stream static pressure (upstream of model)

T_p primary total temperature

T_s secondary total temperature

V_0 free-stream velocity

UNCLASSIFIED

w_p primary weight-flow rate

w_s secondary weight-flow rate

y normal distance from body surface

α divergence angle, deg

β boattail angle, deg

Subscripts:

ab afterburning

l local

nb no afterburning

APPARATUS

Ejector Models

Thirteen different ejectors were used in this investigation, each identified by number. Sketches of the ejectors are presented in figure 1, and each sketch is accompanied with a table of the geometrical parameters. These parameters are also summarized in table I. Ejectors 1 to 12 were mounted on the cylindrical section of the model, which had an 8-inch outside diameter. With ejector 13 the outside diameter of the cylinder was reduced from 8 to 6.4 inches by an abrupt step 22 inches upstream of the exit plane.

Ejectors 1 to 9 and 13 had low boattail angles representative of nacelle-type installations. Ejectors 10 to 12 had high boattail angles as with certain fuselage-type installations.

Ejectors 1 to 9 were investigated with either of two primary-nozzle-exit diameters corresponding to operation with full afterburning and with no afterburning. The ratio of nonafterburning to afterburning primary-nozzle diameter was 0.75.

Ejectors 1 to 6 (figs. 1(a) to (d)) were fixed-geometry types with various values of the geometrical parameters that affect ejector performance (such as expansion ratio, secondary diameter ratio, divergence angle, etc.). All ejectors except ejector 3 were conical. Ejector 3 had a divergent wall contoured (by the method of ref. 1) to produce nearly axial flow at the exit plane.

CONFIDENTIAL

Two modifications of ejector 1 to improve the off-design performance are shown in figure 1(e). They were (1) spoiler rings to encourage jet separation, and (2) air injection through annular slots in the divergent wall to encourage jet separation and to fill in excess flow area at the exit plane. These techniques were investigated independently and also simultaneously.

One type of variable-geometry ejector (7) that was investigated is illustrated in figure 1(f). The divergent portion was assumed to be composed of several leaves that could be rotated in such a manner as to vary the exit area while maintaining a fixed secondary diameter. As flight Mach number (and simultaneously nozzle pressure ratio) decreased, the exit area would be decreased to provide the correct expansion ratio. The two-step boattail geometry that is shown would result in higher boattail drag at Mach 3 than would occur if a single boattail angle had been selected, but it would incur less drag with low-speed positions. An actual variable ejector of this type was not constructed; but rather various positions of the movable portion corresponding to operation at various Mach numbers were selected, and models were constructed to simulate these conditions.

Another variable-geometry ejector (8) that was investigated is shown in figure 1(g). As with ejector 7, the divergent portion was assumed to be constructed of leaves that could be rotated to vary exit area while maintaining a constant secondary diameter. However, in this case the boattail was kept fixed. As a result, as exit area decreased, base area increased. The model was designed with a removable base plate to investigate the effect of base bleed flow. Again, fixed-geometry models were constructed to simulate various positions of interest of the movable portion of the ejector.

A third type of variable-geometry ejector (9) that was investigated is shown in figure 1(h). In this case the boattail and exit area were both fixed and the secondary diameter was variable. The divergent wall was assumed to be constructed of leaves that were hinged at the exit plane. At the design Mach number the secondary diameter would be at its minimum value and would be large enough to permit the passage of the cooling secondary airflow. At lower than design Mach numbers the secondary diameter would be increased to permit the flow of sufficiently large quantities of secondary air to fill in the excess flow area at the exit plane and prevent overexpansion of the primary flow. As with the other variable ejectors, fixed-geometry models simulated positions of interest of the hypothetical variable ejector.

As indicated earlier, ejectors 10 to 12 (figs. 1(i) and (j)) had higher boattail angles than those discussed thus far. They simulated a family of fixed-geometry ejectors with various values of the geometrical parameters. Only one primary-nozzle position (corresponding to full afterburning) was investigated with these models.

Ejector 13 is shown in figure 1(k). It also was a fixed-geometry type, and again only one primary-nozzle position was investigated (that corresponding to full afterburning).

Tunnel Installation

A schematic sketch of the installation of the model in the tunnel is shown in figure 2. The downstream portion of the walls of the 8- by 6-foot test section have been perforated to permit operation at any Mach number from 0.6 to 2.1. The support struts were swept forward 45° to attain a more continuous blockage area distribution for more uniform flow at transonic speeds. Primary and secondary air were ducted separately to the model through the support struts.

Pitot pressure profiles normal to the body just upstream of the boattail are shown in figure 3 for several tunnel Mach numbers. Survey rakes were placed in the plane of the strut and also normal to it. Their axial location is indicated in figure 2. Ignoring unusual distortions of the profiles, it appears that boundary-layer thickness was about 0.8 inch at Mach numbers 2, 1, and 0.8, and about 1.3 inches at Mach 1.35.

Local Mach numbers (denoted by M_l) computed by means of the Rayleigh equation from the local body static pressure and the Pitot pressure farthest from the body are shown in figure 3. These Mach numbers show a circumferential variation that probably was due to the wake from the support strut. At tunnel Mach numbers 2, 1, and 0.8, the local Mach number was lower in the region behind the strut, and at Mach 1.35 it was lower in the plane normal to the strut. The reason for this shift of the low Mach number region as tunnel Mach number is varied is not apparent.

Boattail static-pressure distributions also indicated a varying degree of circumferential variation. This variation was greater at higher tunnel Mach numbers (e.g., Mach 1.35 compared with Mach 0.8) and also generally with higher boattail angles. The worst condition investigated (ejector 5 or 6) is shown in figure 4 at several tunnel Mach numbers. The boattail angle in this case was 7.5°. The region of lowest pressure was behind the strut at Mach 1.35, but at Mach 1 it was in the plane normal to the strut. At Mach 0.8 the pressures were fairly uniform. Although ejectors 10 to 12 had higher over-all boattail angles (in two steps) than ejector 5, the pressures were more uniform. The pressures of other ejectors with lower-angle single-step boattails were also more uniform.

UNCLASSIFIED

PROCEDURE

Experimental Procedure

All ejectors were investigated at several Mach numbers. With ejectors 1 to 12 several values of primary-nozzle pressure ratio were employed at each Mach number, and with each pressure ratio several values of secondary flow were investigated. Only one primary-nozzle pressure ratio with several values of secondary flow was investigated at each Mach number with ejector 13.

For ejectors 1 to 9 full afterburning was assumed for Mach numbers 1.35 and greater, and no afterburning for Mach numbers 1.35 and less. The assumption of the Mach number at which afterburning was turned on did not affect the generality of the conclusions. For ejectors 10 to 13 full afterburning was assumed to occur over the Mach number range of the investigation. Total temperature of both primary and secondary air was about 80° F.

Data Reduction

Weight-flow rates were obtained with standard ASME orifices. Primary total pressure was computed from the primary weight-flow rate and measured static pressures in the primary nozzle upstream of the convergent portion. Secondary total pressure was measured with rakes upstream of the primary-nozzle-exit station.

Because the force-measurement apparatus did not perform with consistent accuracy during the test, ejector gross thrust (exit-plane total momentum) was generally computed from the sum of the total momentum of the primary and secondary streams at reference stations within the ejector plus the sum of wall forces in the axial direction between the reference stations and the exit plane. In general, this procedure gave satisfactory results. Exceptions occurred when large quantities of secondary airflow were used (specifically, the exceptions were ejector 8, Mach 1.35 with no afterburning, and ejector 9, Mach numbers 1.35 and 1.0 with no afterburning). In these cases the thrust computed by this procedure slightly exceeded the maximum theoretical value with the given secondary and primary weight-flow rates and total pressures. This discrepancy is illustrated in figure 5 for ejector 8. At Mach 1.35 (fig. 5(a)) the measured value of adjusted thrust ratio (computed from the gross thrust obtained by the procedure described) exceeded the maximum possible value at very high values of secondary-flow ratio. This did not occur at Mach 1.0 (fig. 5(b)), which was the more typical situation. It is believed that this error was a result of circumferential variations of the secondary flow that were not detected with the instrumentation employed and that became

UNCLASSIFIED

important only when the secondary-flow rate was unusually large. For these exceptional cases, the maximum theoretical values were used in the ANALYSIS section.

With the modified versions of ejector 1 (i.e., with spoilers and with air injection) the wall surfaces were too irregular to evaluate the wall force. Therefore, the data from the force-measurement apparatus (a strain gage and bellows arrangement) were used of necessity. For these configurations the apparatus appeared to be operating reasonably well.

Thrust Ratio

In the ANALYSIS section of the report an effective thrust ratio $(F - m_s V_0 - D)/F_i$ is evaluated that required a knowledge of the gross-thrust ratio F/F_i and the boattail plus base drag D. At some Mach numbers where these data were not obtained, an estimated value for small secondary-flow ratio was computed by the following procedure: (1) If the expansion ratio was correct for the particular nozzle pressure ratio (fully expanded), a 2-percent loss in gross-thrust ratio was assumed to account for friction losses in the nozzle. (2) Additional losses in gross-thrust ratio due to flow divergence at the exit plane were computed assuming $F/F_i = (1 + \cos \alpha)/2$. (3) If the primary flow was underexpanded, the additional loss in gross-thrust ratio was computed from a calculation of exit-plane momentum. (4) If the primary flow was overexpanded, estimates of gross-thrust ratio were made based on earlier unpublished data. (5) Boattail drag was computed from reference 2. (6) The configurations for which these estimates were made did not have bases; therefore, base drag was not needed.

RESULTS

The basic data are presented in figures 6 to 22. Parameters presented are thrust ratio, ejector pressure ratio, boattail drag coefficient, and either base pressure ratio (if a base existed) or exit static-pressure ratio as functions of secondary-flow ratio. The exit static-pressure ratio is useful as an indication whether or not the primary flow is overexpanded.

ANALYSIS

The data of figures 6 to 22 have been used in an analysis of the performance of the ejectors over a Mach number range to obtain a comparison of the solutions considered for the off-design ejector problem. As a basis for comparison, nozzle pressure-ratio schedules with Mach number were assumed as shown in figure 23. Two schedules were used: the schedule for ejectors 1 to 12 is typical of that for engines in use

currently or planned for the near future, and the schedule for ejector 13 is for an advanced, hypothetical, low-pressure-ratio turbojet using a transonic compressor with a design Mach number of 4.

The performance parameter upon which the analysis is based is an effective thrust ratio $(F - m_s V_0 - D)/F_i$, defined as the ejector gross thrust minus the free-stream momentum of secondary air minus the drag of the boattail and base (if there is one) divided by gross thrust of the ideal fully expanded primary flow. With this parameter, configurations designed for a given engine and nacelle size but having different afterbody geometries and secondary flows can be compared directly.

Fixed Geometry and Low Secondary Flow

If a fixed-geometry ejector is designed to provide peak performance at a particular design Mach number, and if off-design performance is not a consideration, then the ejector of necessity must have the correct expansion ratio for that Mach number, and the flow divergence at the exit plane must be small. Ejectors 1 to 3 are of this type with a design Mach number of 3. Assuming that a 2-percent secondary-flow ratio is sufficient for cooling purposes over the Mach number range 0.8 to 3, the performance of these ejectors in this Mach number range is shown in figure 24. Performance of all three ejectors was very poor in the transonic speed range with no afterburning operation. Ejector 2, which had a larger secondary diameter than ejector 1, showed better jet separation characteristics than ejector 1 only at Mach 0.8. The performance of ejector 3 with a contoured divergent wall was about the same as that of the conical ejectors.

The off-design performance of these fixed-geometry ejectors can be improved, at the expense of on-design performance, if the divergence angle is increased or if the expansion ratio is decreased. A higher divergence angle would improve the jet separation characteristics and thus reduce the degree of jet overexpansion (although the pressures in the separated region may still be lower than is desirable because of the base-pressure phenomenon (ref. 3)). With a smaller expansion ratio, the flow would not be as badly overexpanded at off-design conditions.

With ejector 4 the expansion ratio was the correct value for Mach 3 operation, as with ejector 1, but the divergence angle was increased from 9° to 25°. The performance of this ejector is compared with that of ejector 1 in figure 25, again for a flow ratio of 0.02. The high Mach number afterburning performance of ejector 4 was estimated to be somewhat less than that of ejector 1 because of the higher divergence angle, but large improvements in performance occurred at Mach numbers 0.8 and 1.0. However, no improvement was attained at Mach 1.35 with no afterburning. If the afterburning had been continued to some lower Mach number than Mach 1.35 (say Mach 1) with ejector 4, this region of low performance could have been avoided.

With ejectors 5 and 6 the expansion ratio is decreased to that corresponding to complete expansion at Mach 2.2. With 2-percent flow ratio the performances of ejectors 5 and 6 were identical and are also compared with that of ejector 1 in figure 25. Except for the region where underexpansion losses were appreciable (near Mach 3), ejector 5 or 6 provided higher performance than either ejector 1 or 4. The loss in performance of the compromised ejectors (4 to 6) was about the same at Mach 3, but ejectors 5 and 6 were superior at all other Mach numbers. Therefore, it appears that a decreased expansion ratio is a much better compromise than an increased divergence angle.

Fixed Geometry and High Secondary Flow

The reason a fixed-geometry ejector performs poorly at Mach numbers less than design is that the exit area is too large for the available pressure ratio. If the secondary flow were increased sufficiently at this condition, it would fill in the excess exit area and prevent overexpansion of the primary flow. In designing a fixed-geometry ejector that will employ this technique to improve the off-design performance, it is necessary to select a proper value of secondary diameter to optimize over-all performance. It is desirable that there be sufficient secondary flow to prevent primary-flow overexpansion and also that the secondary flow have as high a total pressure as possible so that overall performance will be high. If the secondary diameter is too large for the amount of secondary flow being used, then throttling losses of the secondary air would occur, with an accompanying loss in ejector performance. On the other hand, if the secondary diameter is too small, it may be impossible to pass sufficient air at the available pressure.

The effect of increased secondary flow on off-design ejector performance is shown in figure 26 for ejectors 3 and 6 and for two positions of the variable portions of ejector 9. These data were obtained at Mach 1.35. The secondary diameter ratios were not necessarily the optimum values for the various exit diameter ratios. The effective thrust ratios increased rapidly as flow ratio increased even though full free-stream momentum of the secondary air was charged against the ejector. Thus, large gains would be realized if the drag and weight of the inlet system that provides the additional air can be kept low.

One method of obtaining this additional air is the use of auxiliary inlets. Another method that was considered in detail is the use of the excess air-handling characteristics of a fixed-capture-area main inlet at lower than design speeds. Typical of inlets of this type is the one illustrated in the sketch of figure 27. With this inlet the compression surface is varied at each Mach number so as to maintain an inlet mass-flow ratio of 1, and excess air is disposed of through some sort of bypass system (see ref. 4). For an assumed engine operating with an inlet

of this type, the schedule of bypass mass-flow ratio is shown in figure 27. If it were possible to duct all of this bypass air around the engine and use it in the secondary passage of the ejector (assuming an afterburning primary temperature of 3500° R and a nonafterburning temperature of 1600° R), then maximum available secondary-flow ratio would be as shown in figure 27. Estimating inlet pressure recovery, assuming additional total-pressure losses in ducting the bypass air back to the ejector, and taking the upper schedule of nozzle pressure ratio of figure 23, the maximum available ejector pressure ratio becomes that shown also in figure 27. In the analyses that follow, where secondary air is assumed to be obtained from the inlet bypass, the limits of available weight flow and of available pressure shown in this figure will apply. Mechanical problems of ducting large quantities of high-pressure air around the engine are not considered.

Figure 28 shows the improvement in performance of ejector 6 when large amounts of secondary air are supplied by the inlet bypass. In this case the secondary-flow rate (also shown in the figure) was restricted by the pressure limit. Although the secondary diameter ratio selected for this ejector was not necessarily the optimum, the improvement in performance was large. As discussed earlier, ejector 6 is a compromised version of a Mach 3 ejector (i.e., the expansion ratio is less than ideal at Mach 3). Data at high secondary-flow rates were not obtained with ejectors that were not compromised (e.g., ejector 2), but the beneficial effects of high secondary flow would be obtained with these ejectors also.

The effect on performance of using spoilers with ejector 1 is shown in figure 29. The spoilers were assumed to be retracted for high-speed afterburning operation and extended for transonic nonafterburning operation. At Mach numbers 0.8 and 1 the spoilers caused jet separation as they were intended to do, and hence improved performance relative to the basic unmodified configuration, but failed to do so at Mach 1.35. Even when the jet did separate, however, the pressures in the separated region were still less than p_0 because of the base pressure phenomenon described in reference 3. Thus, performance remained relatively low. Using inlet bypass air, air injection with the spoilers eliminated the loss in performance at Mach 1.35 as shown in the figure, but the resulting performance was no better than that of the basic ejector. At Mach numbers 0.8 and 1 the performance was about the same with air injection plus spoilers as with the spoilers alone. With air injection alone (with the air again supplied by the inlet bypass), about the same improvement in performance was attained at Mach numbers 0.8 and 1 as with the spoilers, but there was no improvement over the basic ejector at Mach 1.35. The secondary-flow rates again were limited by the pressure available.

Although the level of performance was low, a further comparison of the performance of the basic ejector 1 with the performance with air injection is presented in figure 30. At Mach 1.35 (fig. 30(a)) the performance of the basic ejector was higher at a given flow ratio than that with air injection. Therefore, at this Mach number it would be better not to use the air-injection slots and to pass all available secondary air through the secondary passage of the basic ejector. At Mach 1 (fig. 30(b)) slightly higher performance was obtained at a given flow ratio when air injection through the slots was employed. At Mach 0.8 (fig. 30(c)), the performance was higher when the slots were employed, even with zero secondary flow, than with the basic ejector. Increasing secondary flow through the slots produced relatively small improvements in performance. Wall pressure distributions showed that with the slots open the primary flow did not overexpand internally as much as with the basic ejector.

Variable Geometry and Low Secondary Flow

An idealized variable-geometry ejector would have the following features: (1) variable exit diameter to obtain the ideal expansion ratio, (2) variable secondary diameter to produce a divergent shroud for each exit position, (3) variable boattail angle to avoid base area as exit diameter is varied, with leaves sufficiently long that boattail drag is negligible. An exit of this type was not tested, because with the nozzle always on design and with negligible drag the effective thrust ratio is known to be about 0.97.

A simpler version of this exit was investigated and is designated ejector 7. The secondary diameter was kept fixed as exit area varied, and internal and external lines were varied with a single set of leaves that were short, and therefore boattail drag was not negligible. The schedule of exit diameter ratio employed is shown in figure 31. The ejector was designed so that the ideal expansion ratio was attainable for afterburning operation between Mach numbers 1.35 and 3. It was assumed that during the transition from afterburning to nonafterburning operation at Mach number 1.35 the exit area was not changed. This resulted in overexpansion at Mach 1.35 (nonafterburning). At Mach numbers 1 and 0.8, the exit diameter was near the ideal value. However, at Mach numbers 1 and 0.8 the exit diameter was less than the secondary diameter (since the latter was kept fixed), with the result that the shroud was convergent rather than divergent. Such a configuration can have relatively low thrust particularly at low secondary-flow ratios and high primary pressure ratios. Alternatives would be to keep the exit diameter at least as large as the secondary diameter and permit overexpansion (as at Mach 1.35, nonafterburning) or to determine some optimum intermediate exit position. The selection of a different pivot point of the leaves that would permit secondary diameter to vary as the leaves rotated might avoid this problem.

The performance of ejector 7 is presented in figure 32 for 2-percent flow ratio. Also shown for reference is the estimated performance of the ideal variable ejector described earlier. Although ejector 7 would have the ideal expansion ratio at Mach 3, its performance will be less than that of the ideal ejector because of the boattail drag. Its relatively low performance at Mach numbers 1.35 and 1 (nonafterburning) was due to overexpansion and to the convergent shroud, respectively.

Another ejector that also was mechanically simpler than the ideal variable ejector was ejector 8. The secondary diameter and also the boattail were fixed. The schedule of exit diameter ratio employed with this ejector is shown in figure 33. The flow was slightly underexpanded at Mach 3 in order to alleviate the off-design problem somewhat. The diameter ratio was near the ideal value at Mach numbers between 2 and 1.35. For this ejector the exit diameter was never less than the value of the secondary diameter in order to avoid the problem of the convergent shroud. The shroud became cylindrical at Mach 1.35 and remained so at all Mach numbers less than that. This resulted in overexpansion for nonafterburning operation.

The performance of ejector 8 with 2-percent flow ratio (without base flow) is presented in figure 34. Again the performance of the ideal ejector is presented as a reference. At Mach 3 it is estimated that the performance of ejector 8 would be less than that of the ideal ejector because the flow is slightly underexpanded and because of boattail drag. At transonic speeds the performance is lower because of (1) overexpansion, (2) boattail drag, and (3) base drag.

Variable Geometry and High Secondary Flow

The improvement in performance of ejector 8 by employing large amounts of base flow to eliminate the base drag is also shown in figure 34. It was assumed that the air was provided by the inlet bypass. The drop in performance for nonafterburning operation was due partly to overexpansion of the primary flow and also to the total-pressure losses of the secondary flow.

Ejector 9 also was simpler than the ideal variable ejector in that the exit area and the boattail were fixed. The schedule of secondary diameter ratio that was employed is presented in figure 35. By means of extrapolated data and one-dimensional-flow calculations, these values of diameter ratio were selected as those that would match the available bypass flow schedule satisfactorily. The performance of this ejector is presented in figure 36. As described in the Data Reduction section, the measured values of thrust ratio exceeded the theoretically maximum possible value for nonafterburning operation. The theoretical values are

shown in figure 36 where this problem occurred. The performance at Mach 3 again would be less than that of the ideal ejector because of boattail drag and because the flow was slightly underexpanded ($d_e/d_p = 1.6$). The drop in performance for nonafterburning operation occurred because the secondary total pressure was less than free-stream total pressure as a result of the losses assumed in the maximum-pressure-ratio schedule of figure 27.

Comparison

The best performing ejectors of those considered thus far are compared in figure 37. The performance of fixed-geometry ejector 6 with high secondary flow was within the range of performance encompassed by the more complex variable-geometry ejectors. The highest performance in the low Mach number range was obtained with ejector 9.

Ejectors with Full Afterburning

Ejectors 10 to 13 were investigated with full afterburning over the entire speed range. The supersonic performance of ejectors 10 to 12 has been obtained in an earlier investigation, and the speed range is extended into the transonic range in the present report. The performance of these ejectors based on the same pressure-ratio schedule as that of the previous ejectors is shown in figure 38 for 2-percent flow ratio. Ejector 10, which differed from ejector 11 only in that it had a smaller secondary diameter, had about the same performance as ejector 11. Because these ejectors had high boattail angles representative of some fuselage-type installations, boattail drag was high, and thus the general level of performance was low. Ejector 12 had a higher expansion ratio (corresponding to complete expansion at Mach 3) than ejectors 10 and 11. For a given engine and fuselage size, an increase in expansion ratio would result in an increase in exit area and hence a reduction in boattail area. The increased overexpansion losses with the higher expansion ratio at off-design conditions would at least be partly compensated for by the decreased boattail drag. However, because of details of model construction, ejector 12 had a smaller primary-nozzle area than ejectors 10 and 11; whereas exit area, fuselage area, and boattail geometry were identical. Hence the data of figure 38 do not show the net effect of a simple change in expansion ratio, but rather show the effect of Mach number on the performance of various ejector geometries. As with ejectors 10 and 11, the level of performance of ejector 12 was low because of high boattail drag, but additional losses occurred with ejector 12 because of the greater degree of overexpansion of the primary flow.

The effect of secondary flow on the performance of ejectors 10 to 12 at Mach 1 is shown in figure 39. Again, appreciable increases in performance occurred as flow ratio increased.

The effect of secondary flow on the performance of ejector 13 is shown in figure 40. The nozzle-pressure-ratio schedule was lower than that for the previous nozzles (see fig. 23). The magnitude of the increase in performance as a result of increasing the flow ratio differed with Mach number but was appreciable at all Mach numbers. The greatest improvement occurred at Mach 1.5.

SUMMARY OF RESULTS

The off-design performance of fixed- and variable-geometry divergent ejectors has been investigated. The ejectors were designed for turbojet operation at Mach 3 and were investigated in the Mach number range 0.8 to 2. The following results were obtained:

1. Large performance losses occurred at off-design Mach numbers with simple fixed-geometry ejectors designed for peak performance at Mach 3.

2. Compromising design performance by increasing the divergence angle or by decreasing the expansion ratio produced large gains in off-design performance. A decreased expansion ratio was a better compromise than an increased divergence angle.

3. Increasing the secondary airflow to fill in the excess exit area of fixed-geometry ejectors at off-design conditions produced large gains in performance and made them competitive with fairly complex variable-geometry types.

4. Variable-expansion-ratio ejectors with compromises to reduce mechanical complexity produced performance reasonably close to that of an ideal variable ejector.

5. An ejector with a fixed exit area and a variable secondary diameter with high secondary airflow produced the best performance of the types investigated.

Lewis Flight Propulsion Laboratory
National Advisory Committee for Aeronautics
Cleveland, Ohio, July 15, 1958

REFERENCES

1. Clippinger, R. F.: Supersonic Axially Symmetric Nozzles. Rep. No. 794, Ballistic Res. Labs., Aberdeen Proving Ground, Dec. 1951.

2. Jack, John R.: Theoretical Pressure Distributions and Wave Drags for Conical Boattails. NACA TN 2972, 1953.

3. Baughman, L. Eugene, and Kochendorfer, Fred D.: Jet Effects on Base Pressures of Conical Afterbodies at Mach 1.91 and 3.12. NACA RM E57E06, 1957.

4. Gertsma, L. W., and Beheim, M. A.: Performance at Mach Numbers 3.07, 1.89, and 0 of Inlets Designed for Inlet-Engine Matching Up to Mach 3. NACA RM E58B13, 1958.

CONFIDENTIAL

TABLE I. - SUMMARY OF EJECTOR GEOMETRIES

Ejector	$\frac{d_e}{d_{p,ab}}$	$\frac{d_s}{d_{p,ab}}$	$\frac{l}{d_{p,ab}}$	β, deg	α, deg	$\frac{d_{p,np}}{d_{p,ab}}$	$\frac{d_m}{d_{p,ab}}$	$\frac{d_B}{d_{p,ab}}$
1	1.8	1.05	2.37	2	9	0.75	2.0	1.8
2	1.8	1.21	2.37	2	7	0.75	2.0	1.8
3	1.75	1.05	2.37	2	Contoured	0.75	2.0	1.78
4	1.8	1.05	0.875	3.5	23	0.75	2.0	1.8
5	1.45	1.05	1.26	7.5	9	0.75	2.0	1.45
6	1.45	1.21	1.26	7.5	6.5	0.75	2.0	1.45
7	1.8 (at M = 3)	1.05	1.5	$\beta_1 = 7$ $\beta_2 = -11.5$ (at M = 3)	14 (at M = 3)	0.75	2.0	1.8 (at M = 3)
8	1.6 (at M = 3)	1.05	1.69	6.5	9.5 (at M = 3)	0.75	2.0	1.6
9	1.6	1.05 (at M = 3)	1.69	5	9.5 (at M = 3)	0.75	2.0	1.6
10	1.45	1.09	0.8	$\beta_1 = 5$ $\beta_2 = 7.5$	12.5	1.0	2.5	1.5
11	1.45	1.21	0.8	$\beta_1 = 5$ $\beta_2 = 7.5$	8.5	1.0	2.5	1.5
12	1.81	1.21	1.9	$\beta_1 = 5$ $\beta_2 = 7.5$	9	1.0	3.08	1.85
13	1.45	1.15	0.82	0	10.5	1.0	1.45	1.45

CONFIDENTIAL

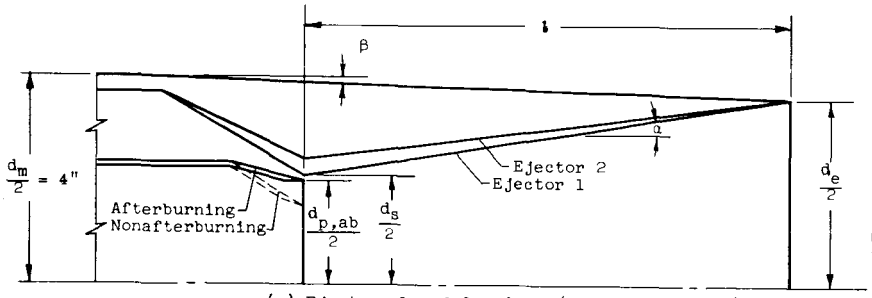

(a) Ejectors 1 and 2: $d_{p,nb}/d_{p,ab} = 0.75$; $d_m/d_{p,ab} = 2.0$.

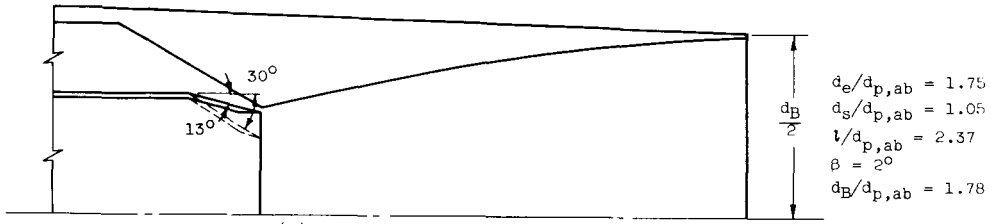

(b) Ejector 3: $d_{p,nb}/d_{p,ab} = 0.75$; $d_m/d_{p,ab} = 2.0$.

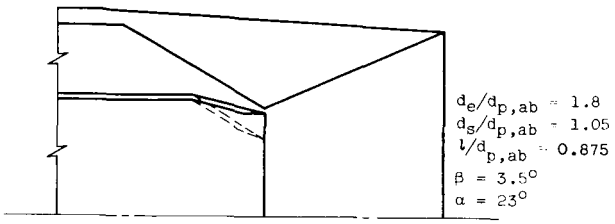

(c) Ejector 4: $d_{p,nb}/d_{p,ab} = 0.75$; $d_m/d_{p,ab} = 2.0$.

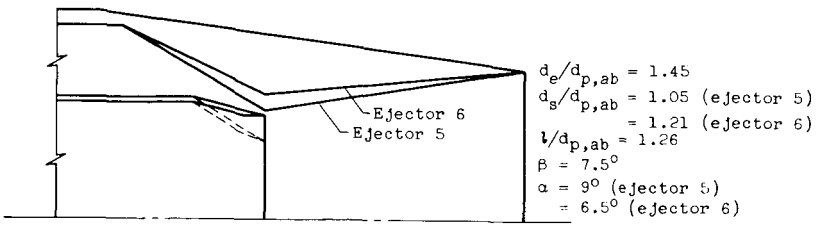

(d) Ejectors 5 and 6: $d_{p,nb}/d_{p,ab} = 0.75$; $d_m/d_{p,ab} = 2.0$.

Figure 1. - Ejector geometries.

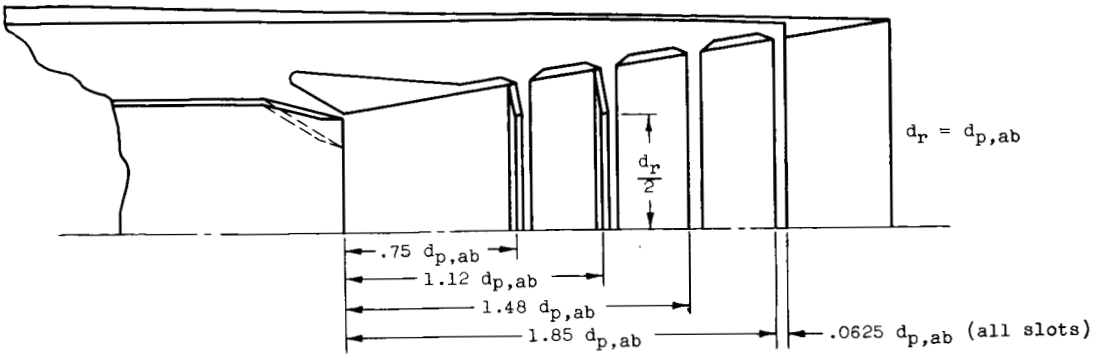

(e) Ejector 1 with spoilers and air injection.

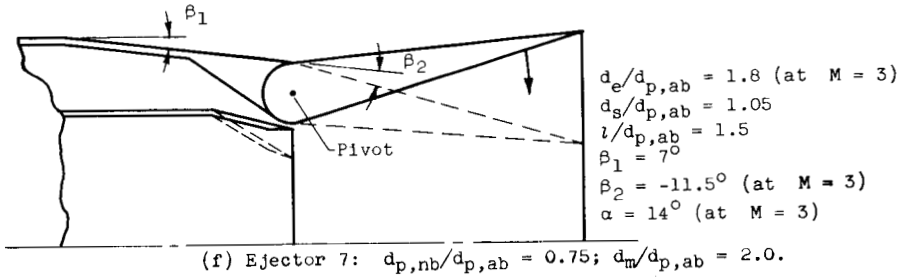

(f) Ejector 7: $d_{p,nb}/d_{p,ab} = 0.75$; $d_m/d_{p,ab} = 2.0$.

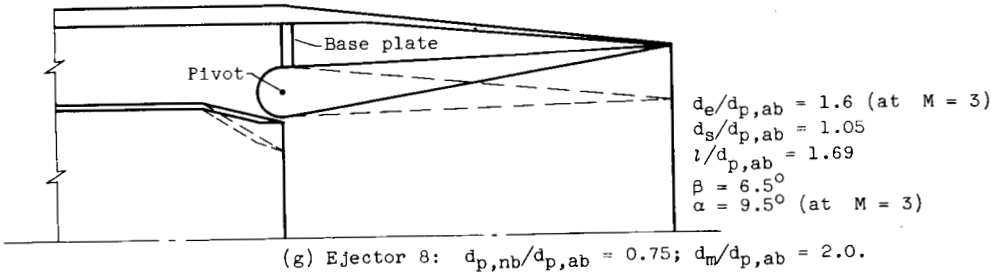

(g) Ejector 8: $d_{p,nb}/d_{p,ab} = 0.75$; $d_m/d_{p,ab} = 2.0$.

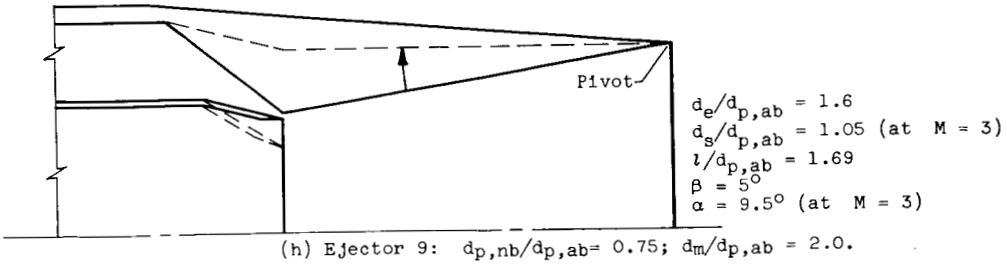

(h) Ejector 9: $d_{p,nb}/d_{p,ab} = 0.75$; $d_m/d_{p,ab} = 2.0$.

Figure 1. - Continued. Ejector geometries.

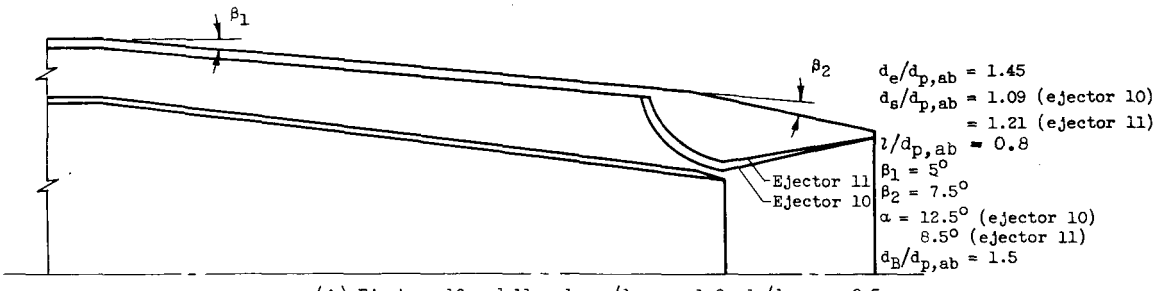

(i) Ejectors 10 and 11: $d_{p,nb}/d_{p,ab} = 1.0$; $d_m/d_{p,ab} = 2.5$.

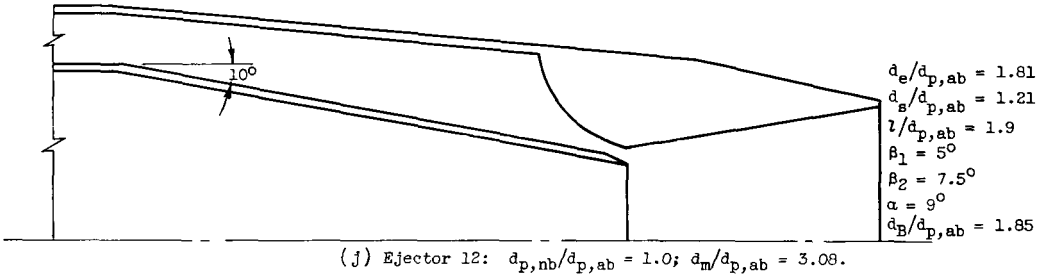

(j) Ejector 12: $d_{p,nb}/d_{p,ab} = 1.0$; $d_m/d_{p,ab} = 3.08$.

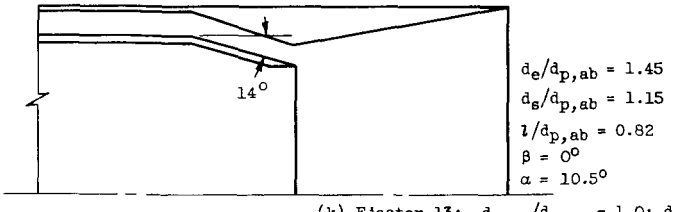

(k) Ejector 13: $d_{p,nb}/d_{p,ab} = 1.0$; $d_m/d_{p,ab} = 1.45$.

Figure 1. - Concluded. Ejector geometries.

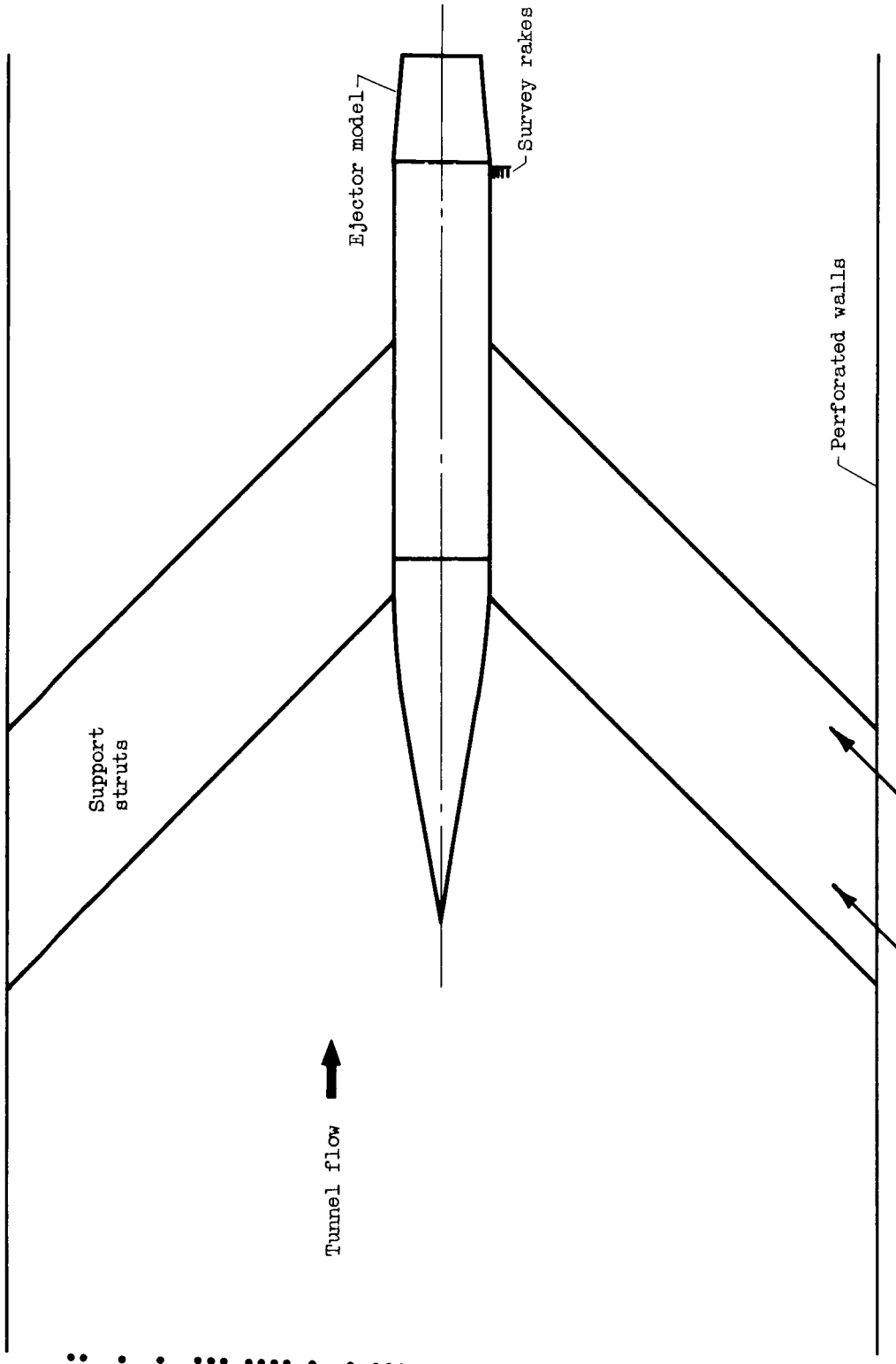

Figure 2. - Tunnel installation.

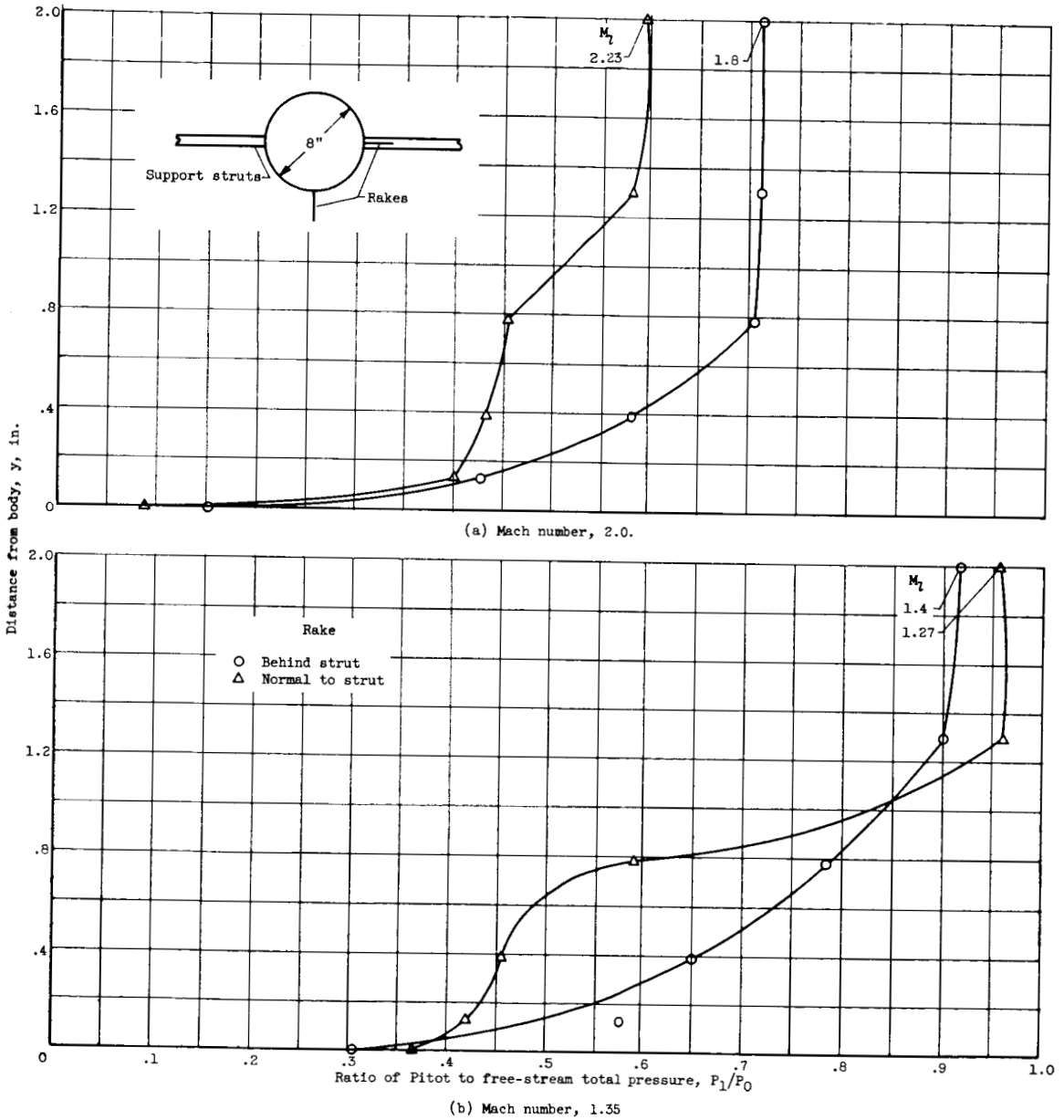

(a) Mach number, 2.0.

(b) Mach number, 1.35

Figure 3. - Pitot pressure profiles upstream of boattail.

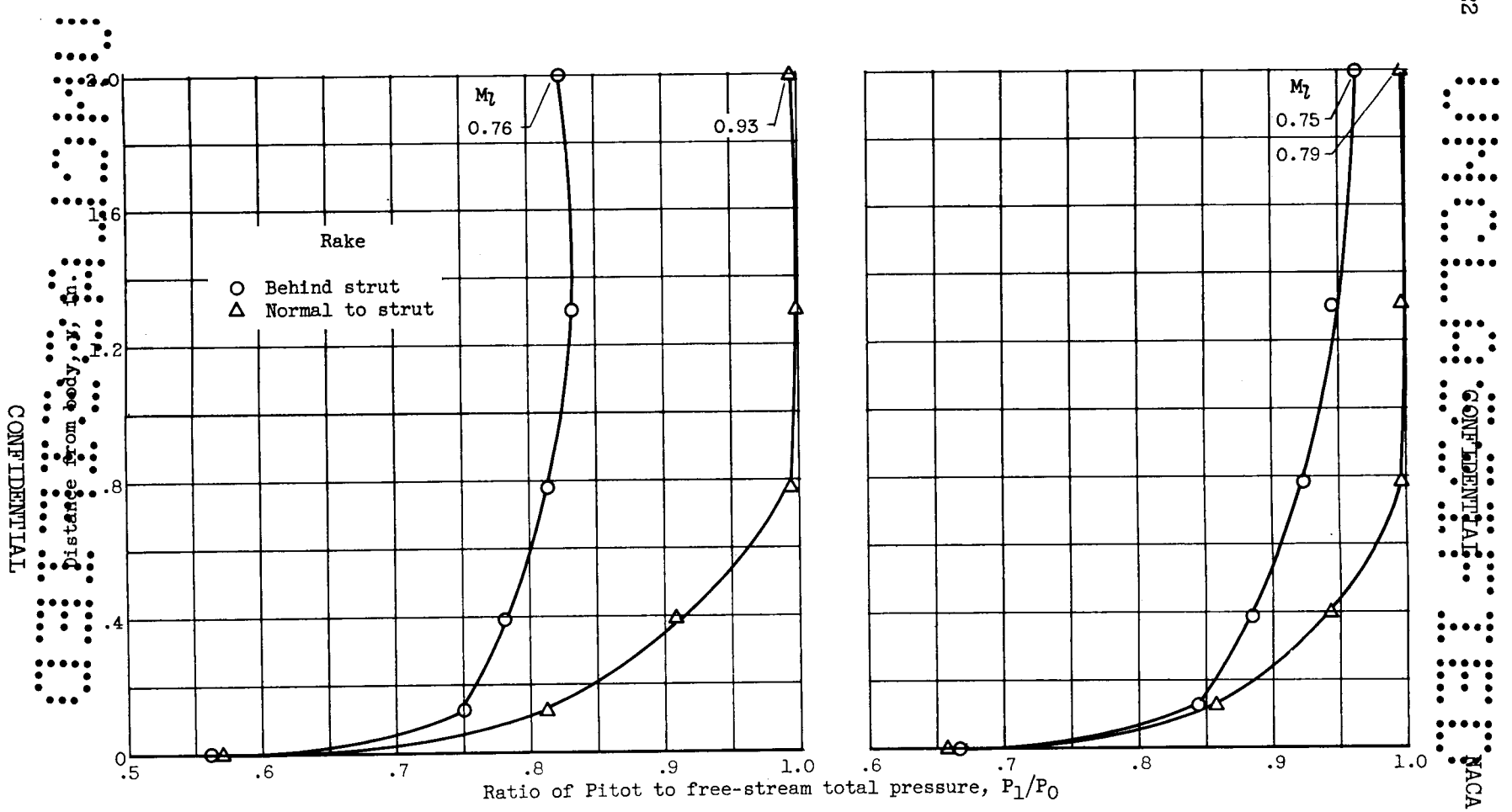

(c) Mach number, 1.0.

(d) Mach number, 0.8.

Figure 3. - Concluded. Pitot pressure profiles upstream of boattail.

CONFIDENTIAL

CONFIDENTIAL

UNCLASSIFIED

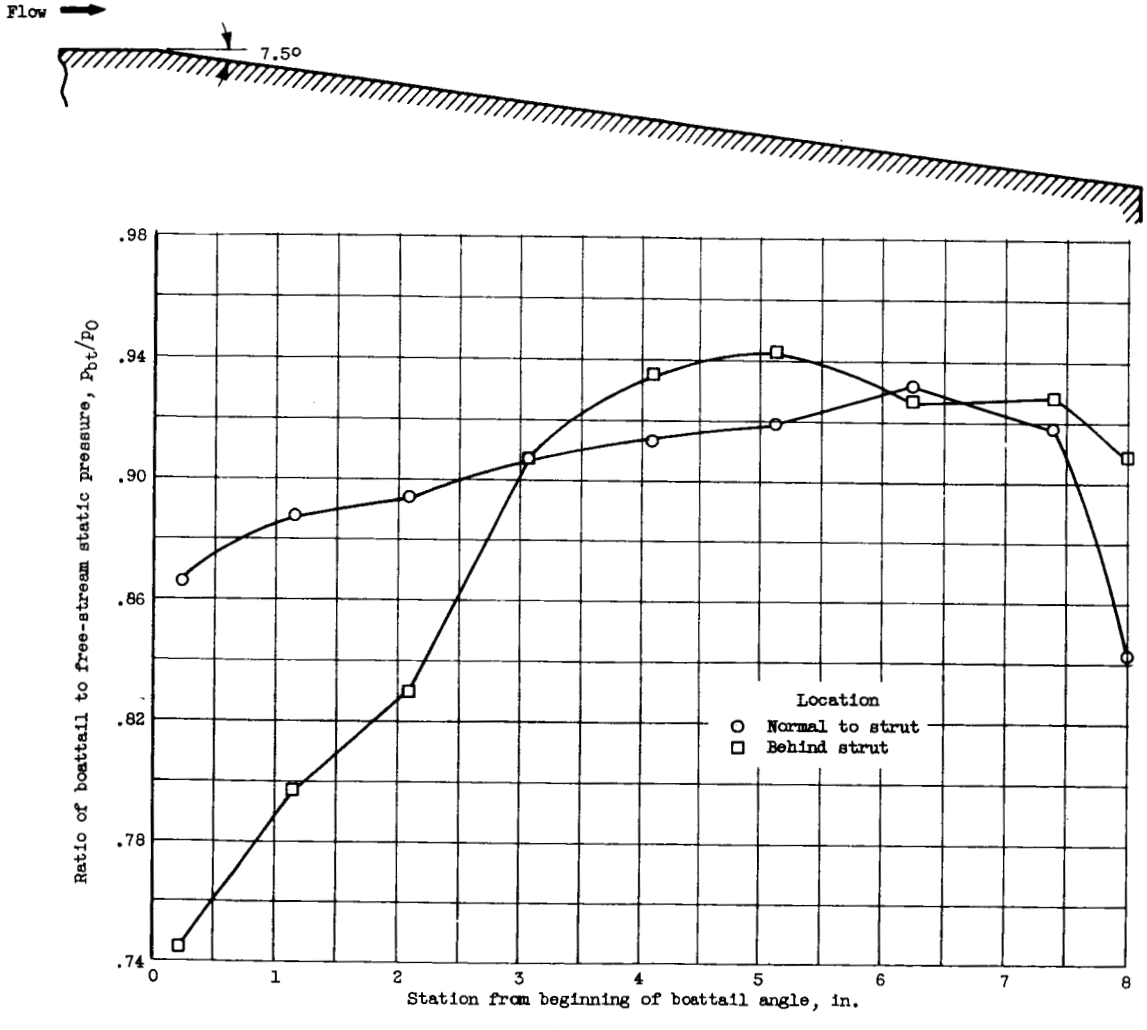

(a) Mach number, 1.35.

Figure 4. - Boattail static-pressure distribution with 7.5° boattail angle.

UNCLASSIFIED

UNCLASSIFIED

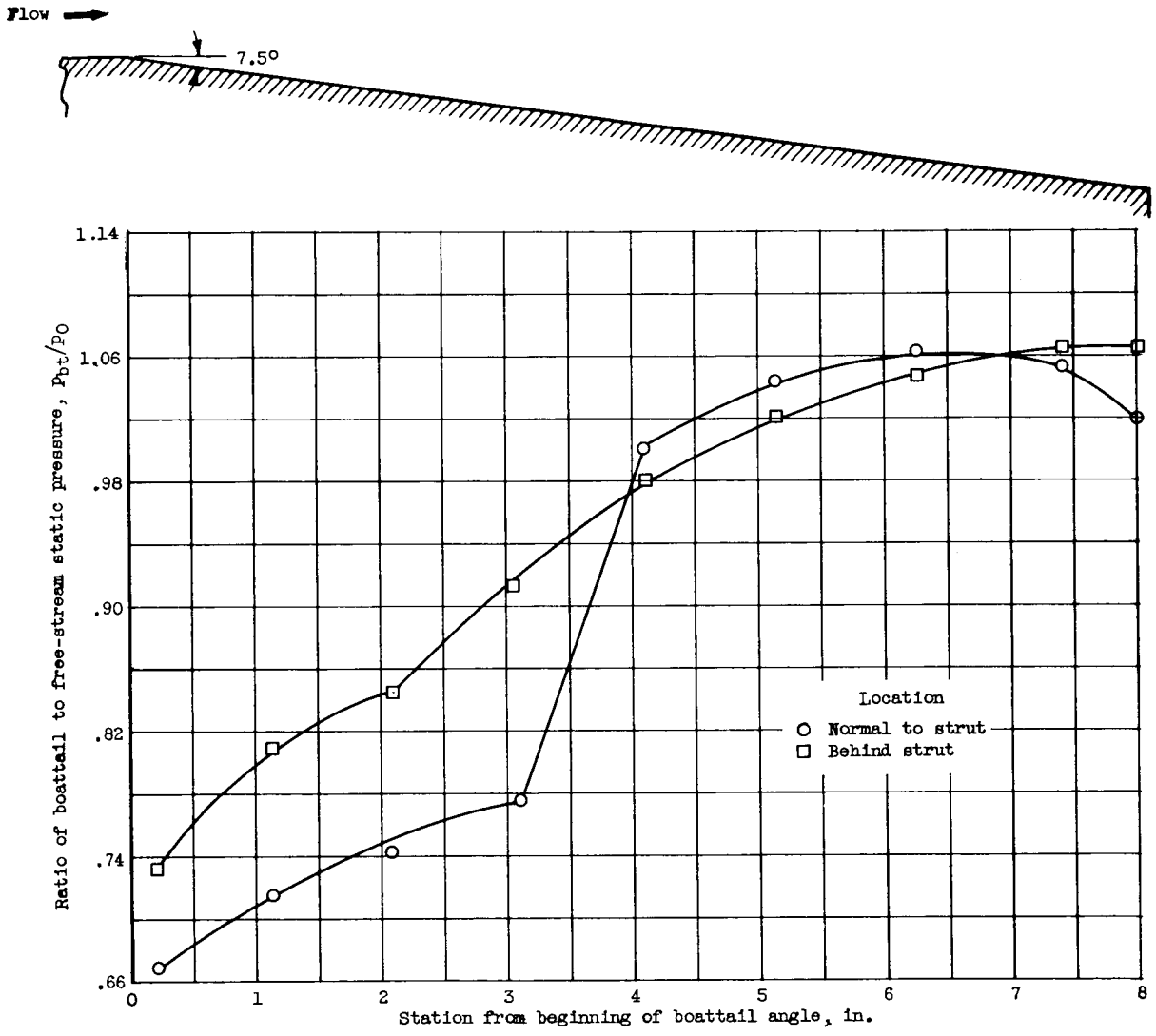

(b) Mach number, 1.0.

Figure 4. - Continued. Boattail static-pressure distribution with 7.5° boattail angle.

UNCLASSIFIED

CONFIDENTIAL

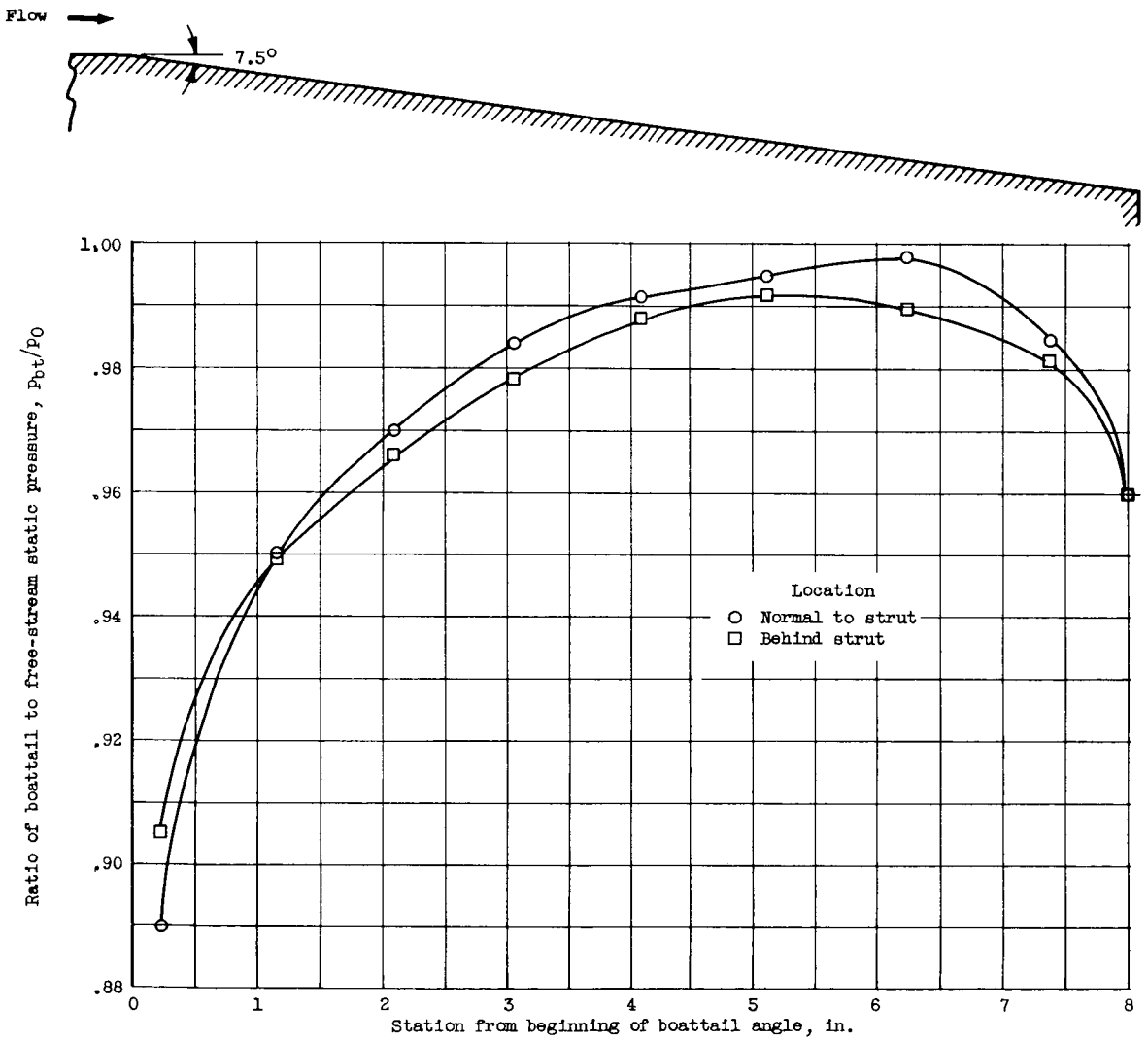

(c) Mach number, 0.8.

Figure 4. - Concluded. Boattail static-pressure distribution with 7.5° boattail angle.

CONFIDENTIAL

UNCLASSIFIED

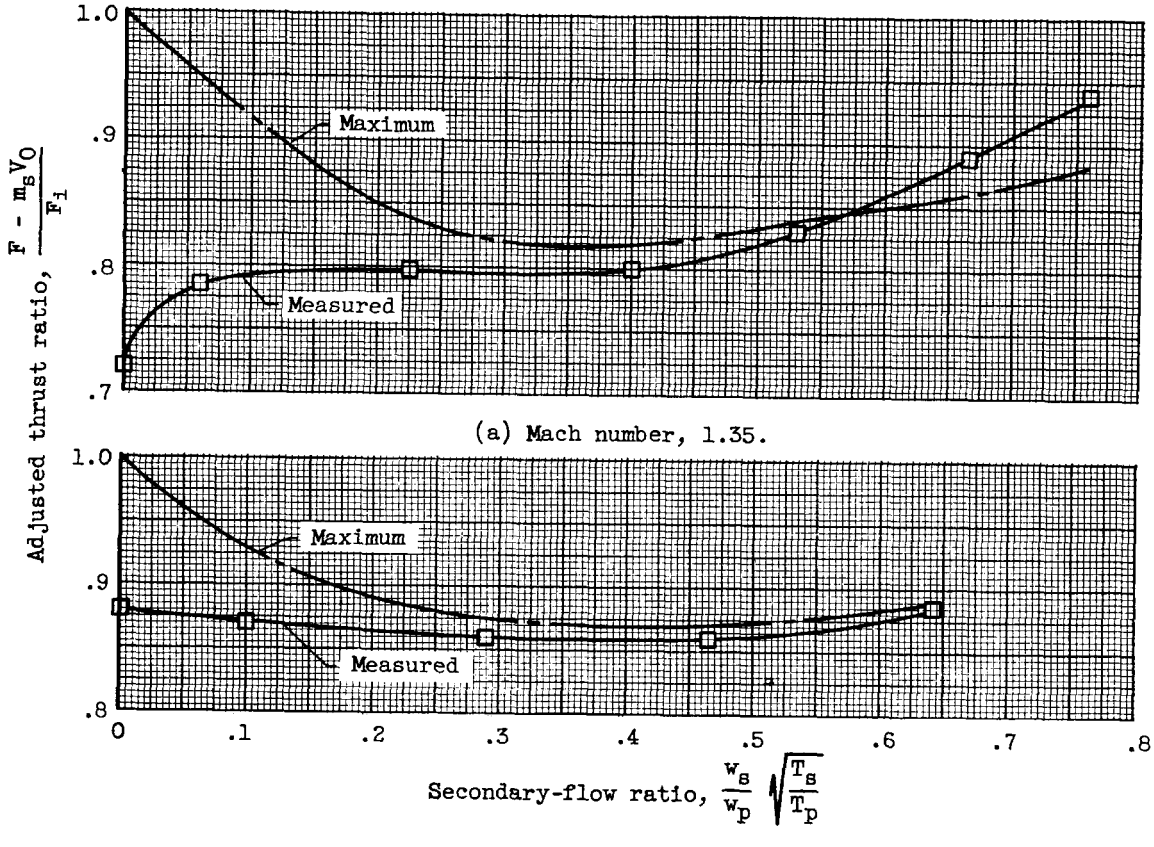

Figure 5. - Comparison of measured and maximum thrust ratios for ejector 8 with no afterburning.

UNCLASSIFIED

UNCLASSIFIED

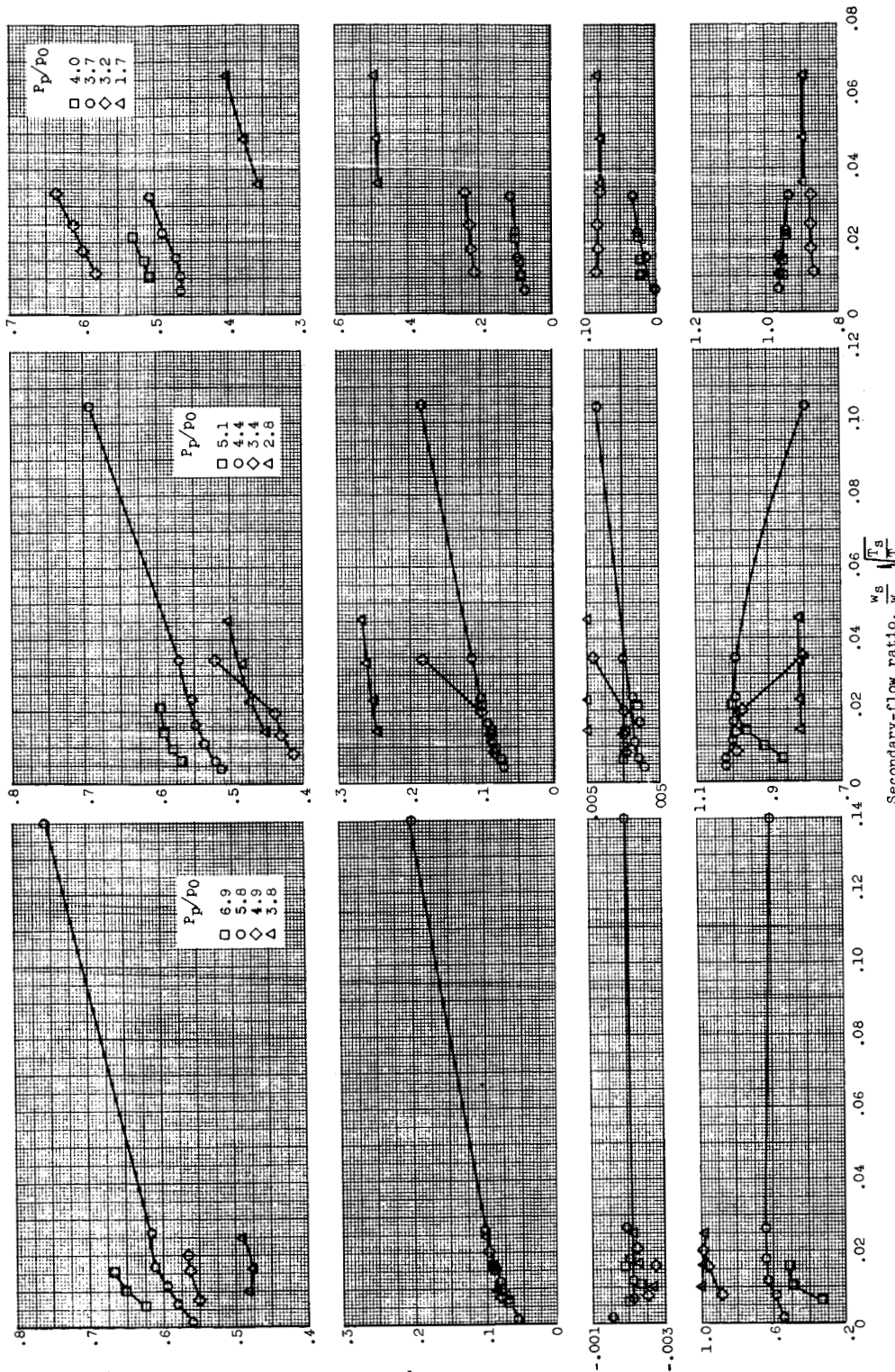

(a) No afterburning; Mach number, 1.35.

(b) No afterburning; Mach number, 1.0.

(c) No afterburning; Mach number, 0.8.

Figure 6. - Performance of ejector 1.

CONFIDENTIAL

UNCLASSIFIED

UNCLASSIFIED

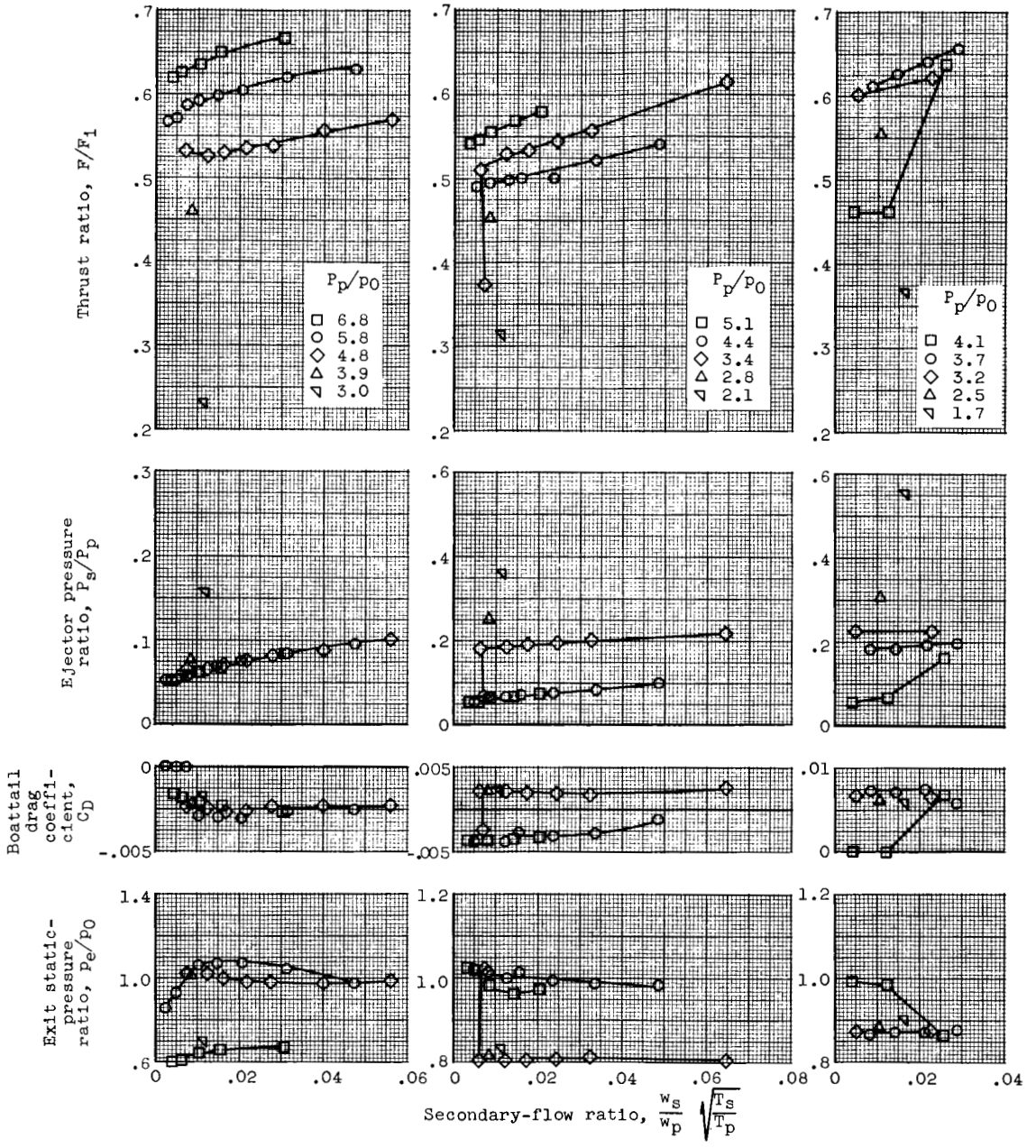

(a) No afterburning; Mach number, 1.35.

(b) No afterburning; Mach number, 1.0.

(c) No afterburning; Mach number, 0.8.

Figure 7. - Performance of ejector 2.

UNCLASSIFIED

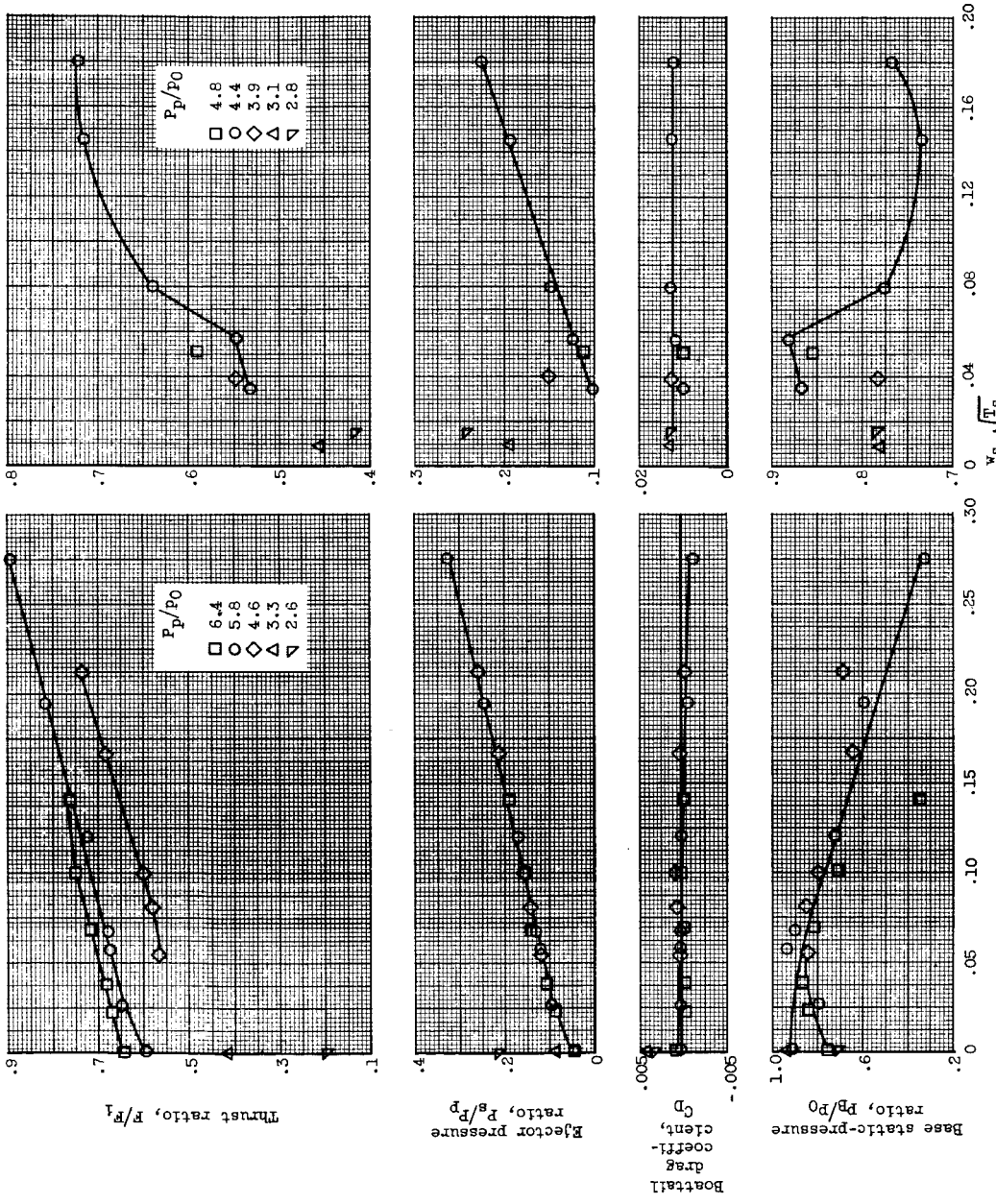

(a) No afterburning; Mach number, 1.35. (b) No afterburning; Mach number, 1.0.

Figure 8. - Performance of ejector 3.

UNCLASSIFIED

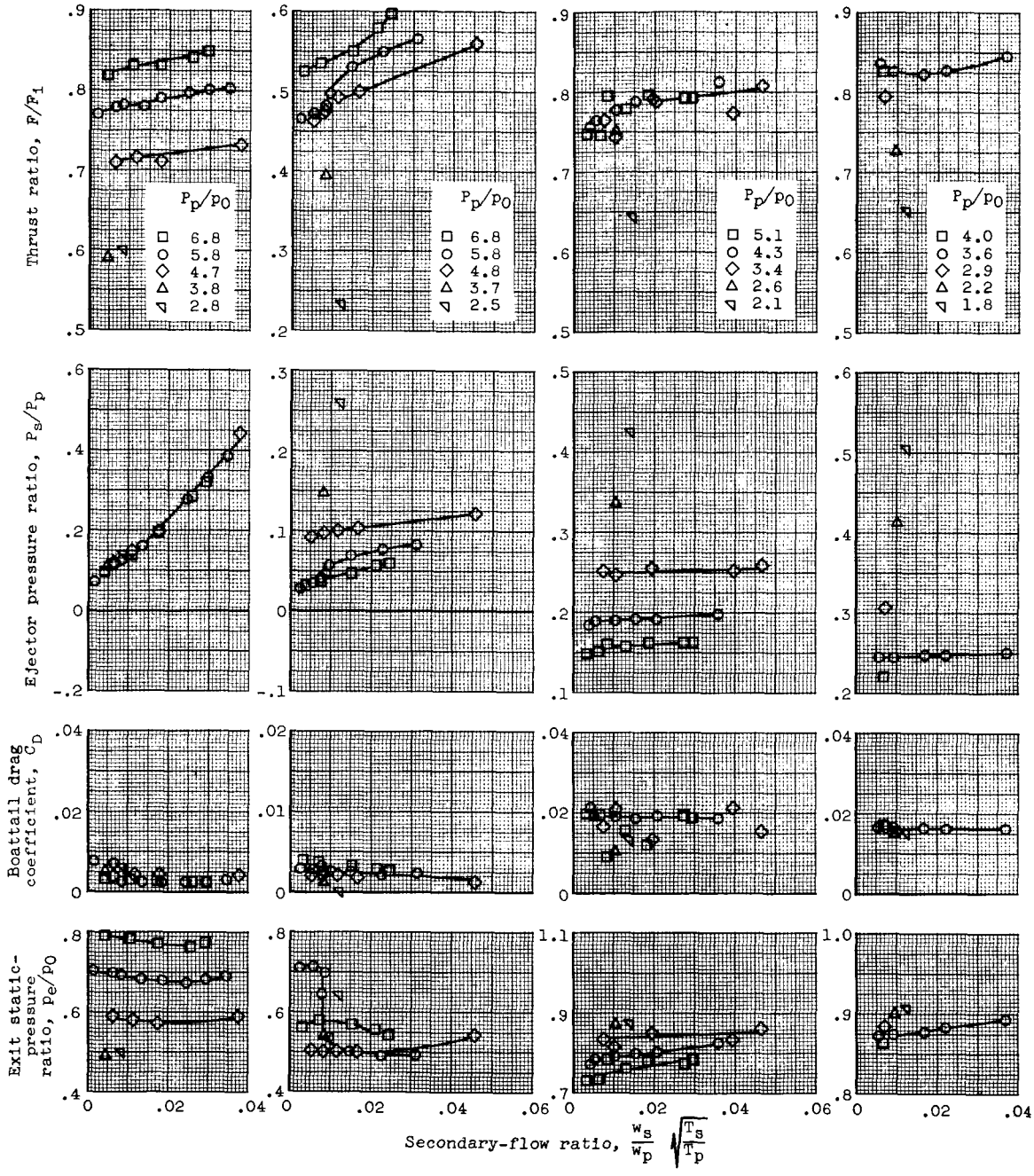

(a) Afterburning; Mach number, 1.35.

(b) No afterburning; Mach number, 1.35.

(c) No afterburning; Mach number, 1.0.

(d) No afterburning; Mach number, 0.8.

Figure 9. - Performance of ejector 4.

UNCLASSIFIED

CLASSIFICATION

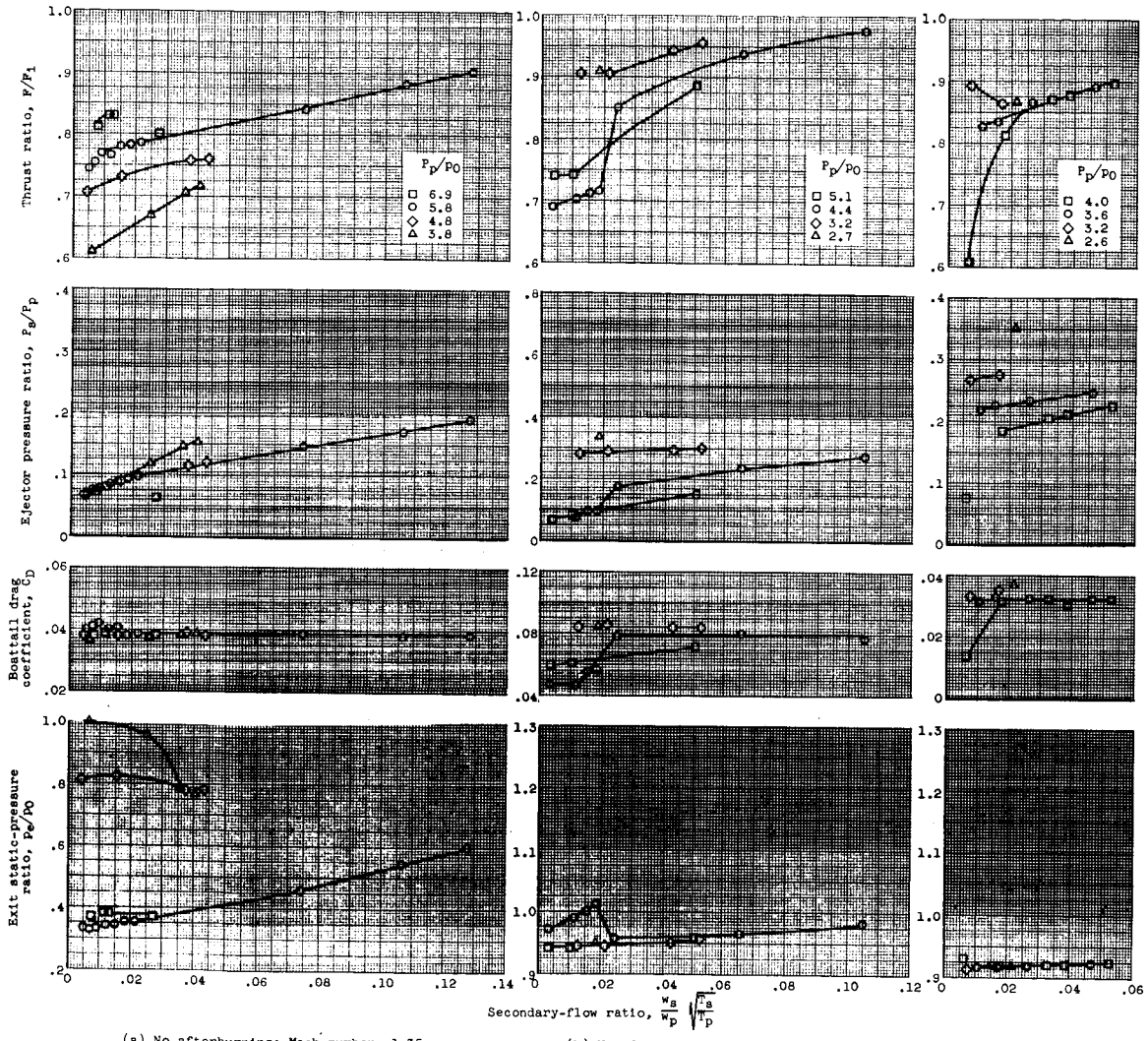

(a) No afterburning; Mach number, 1.35. (b) No afterburning; Mach number, 1.0. (c) No afterburning; Mach number, 0.8.

Figure 10. - Performance of ejector 5.

CLASSIFICATION

UNCLASSIFIED

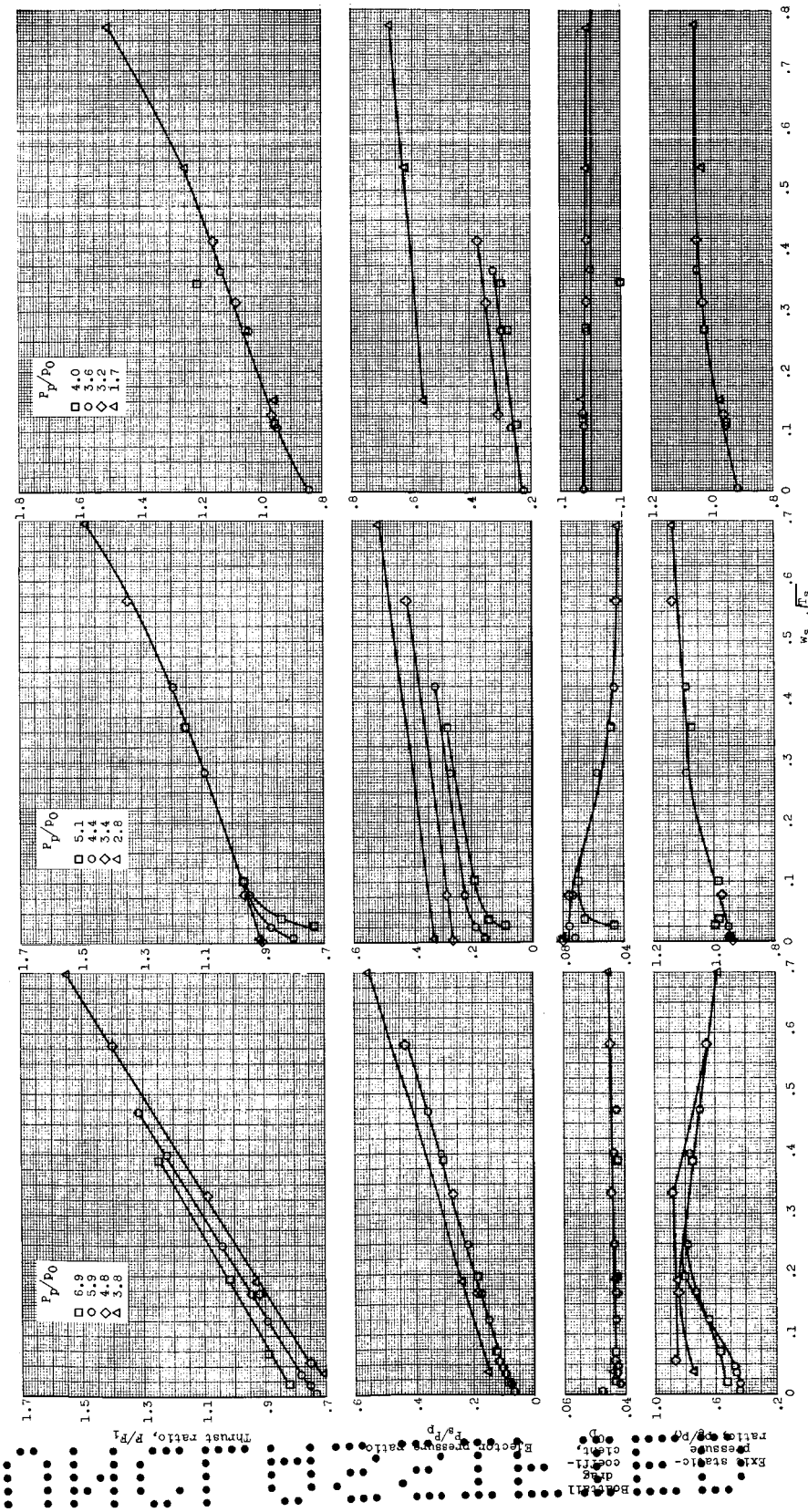

(a) No afterburning; Mach number, 1.35. (b) No afterburning; Mach number, 1.0. (c) No afterburning; Mach number, 0.8.

Figure 11. - Performance of ejector 6.

UNCLASSIFIED

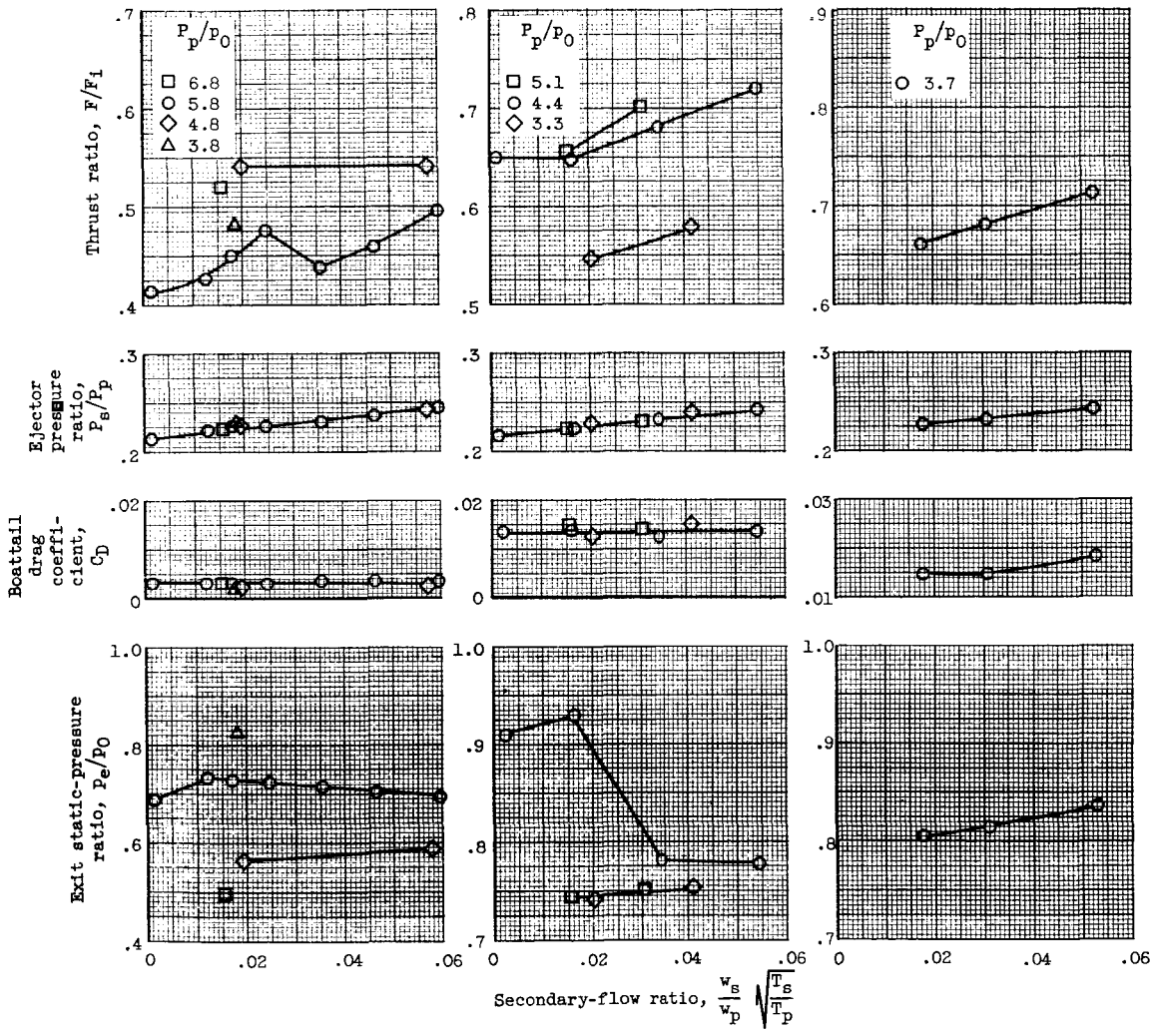

(a) No afterburning; Mach number, 1.35.

(b) No afterburning; Mach number, 1.0.

(c) No afterburning; Mach number, 0.8.

Figure 12. - Performance of ejector 1 with spoilers.

UNCLASSIFIED

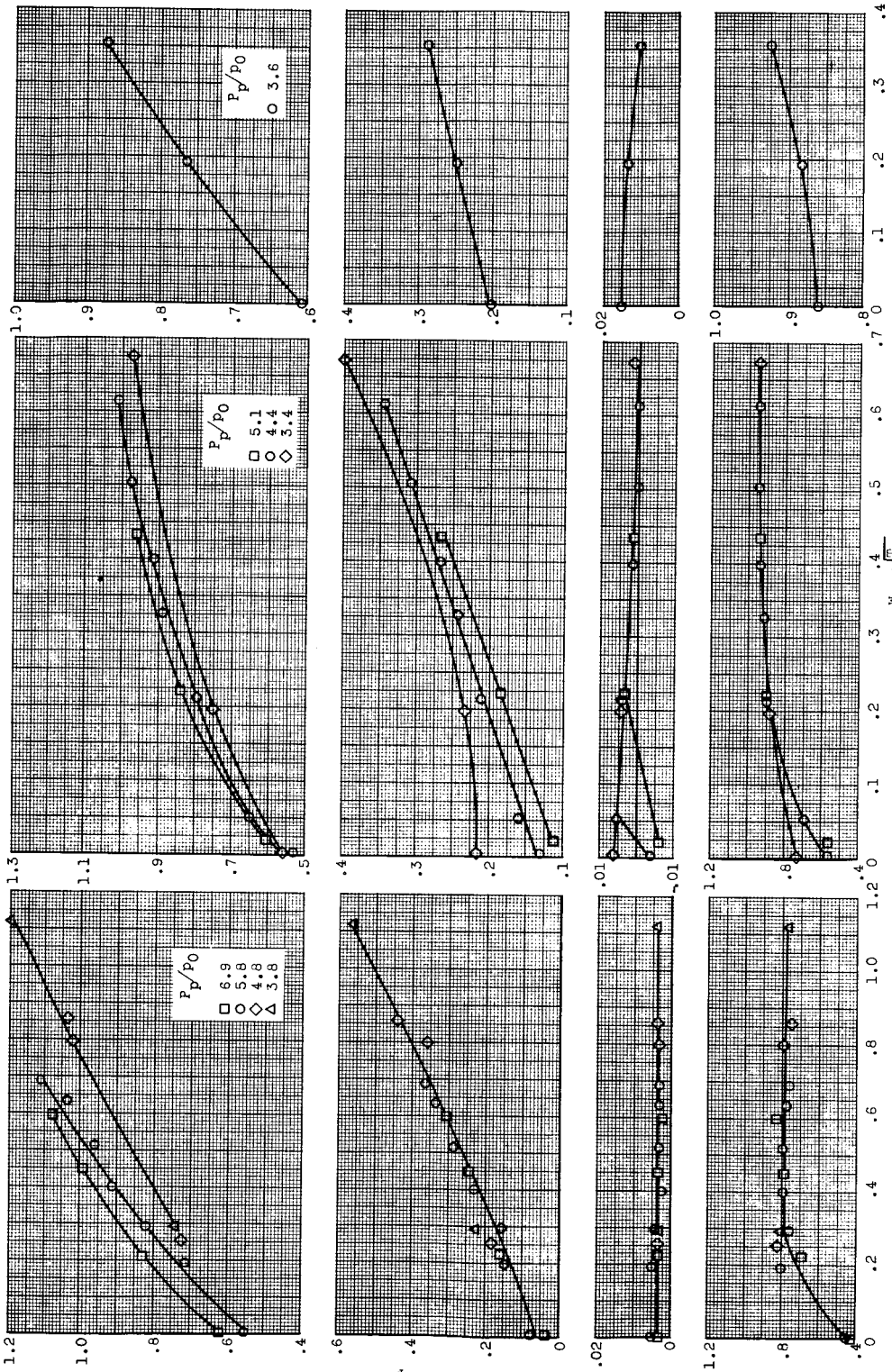

(a) No afterburning; Mach number, 1.35.

(b) No afterburning; Mach number, 1.0.

(c) No afterburning; Mach number, 0.8.

Figure 13. - Performance of ejector 1 with air injection.

UNCLASSIFIED

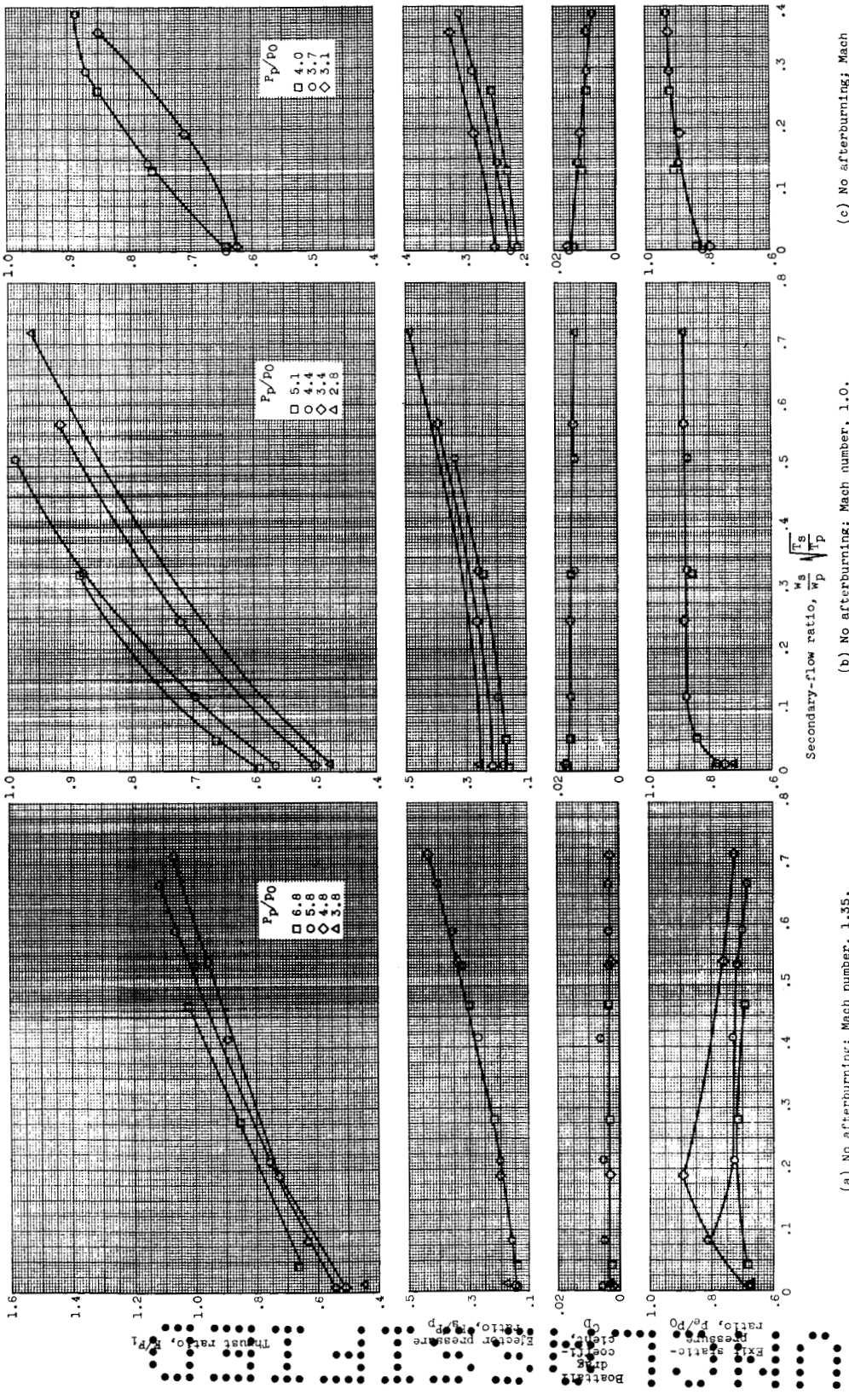

(a) No afterburning; Mach number, 1.35.

(b) No afterburning; Mach number, 1.0.

(c) No afterburning; Mach number, 0.8.

Figure 14. - Performance of ejector 1 with spoilers and air injection.

UNCLASSIFIED

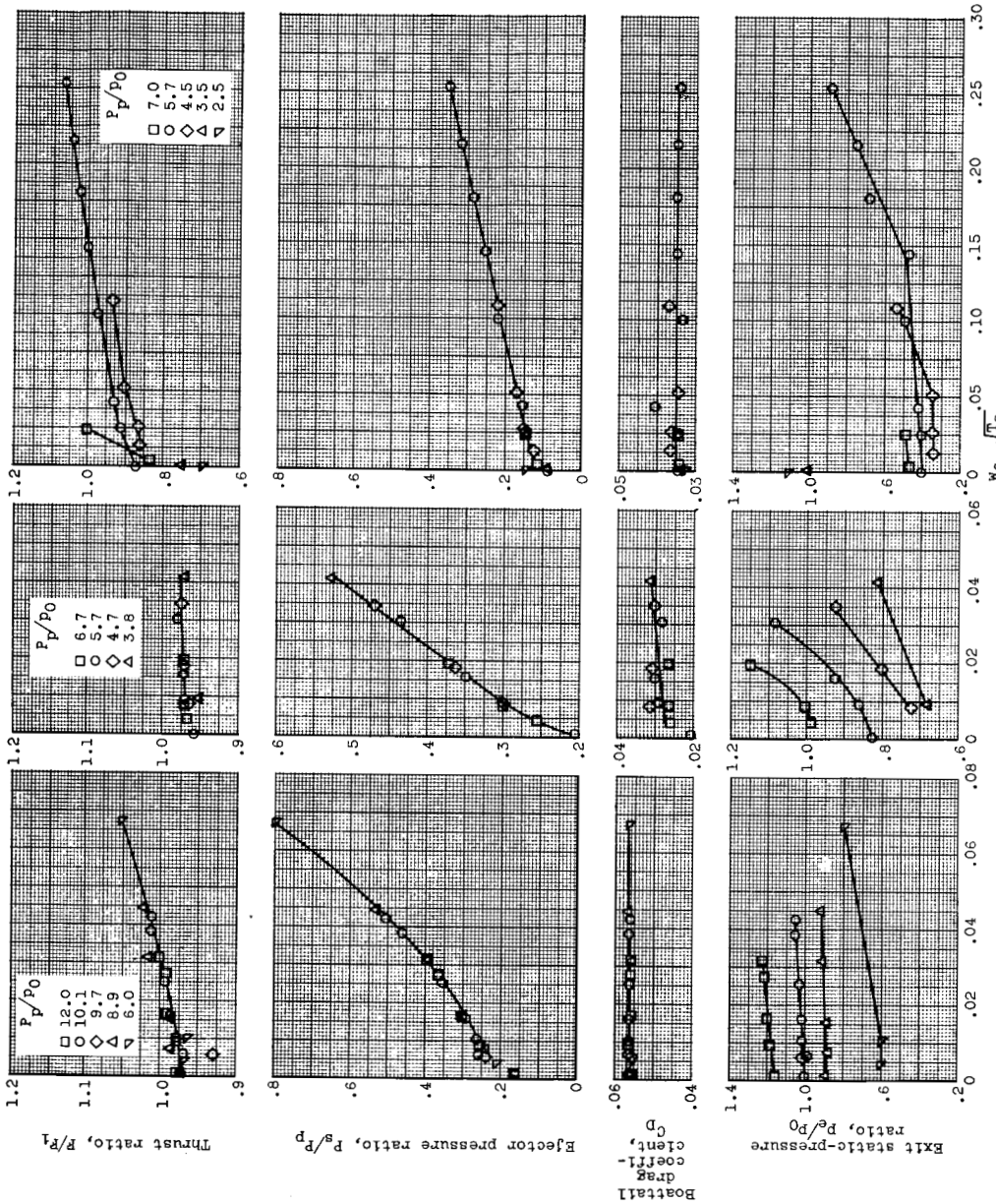

(a) Afterburning; Mach number, 2.0; d_e/d_p, 1.4.

(b) Afterburning; Mach number, 1.35; d_e/d_p, 1.2.

(c) No afterburning; Mach number, 1.35; d_e/d_p, 1.6.

Figure 15. - Performance of ejector 7.

UNCLASSIFIED

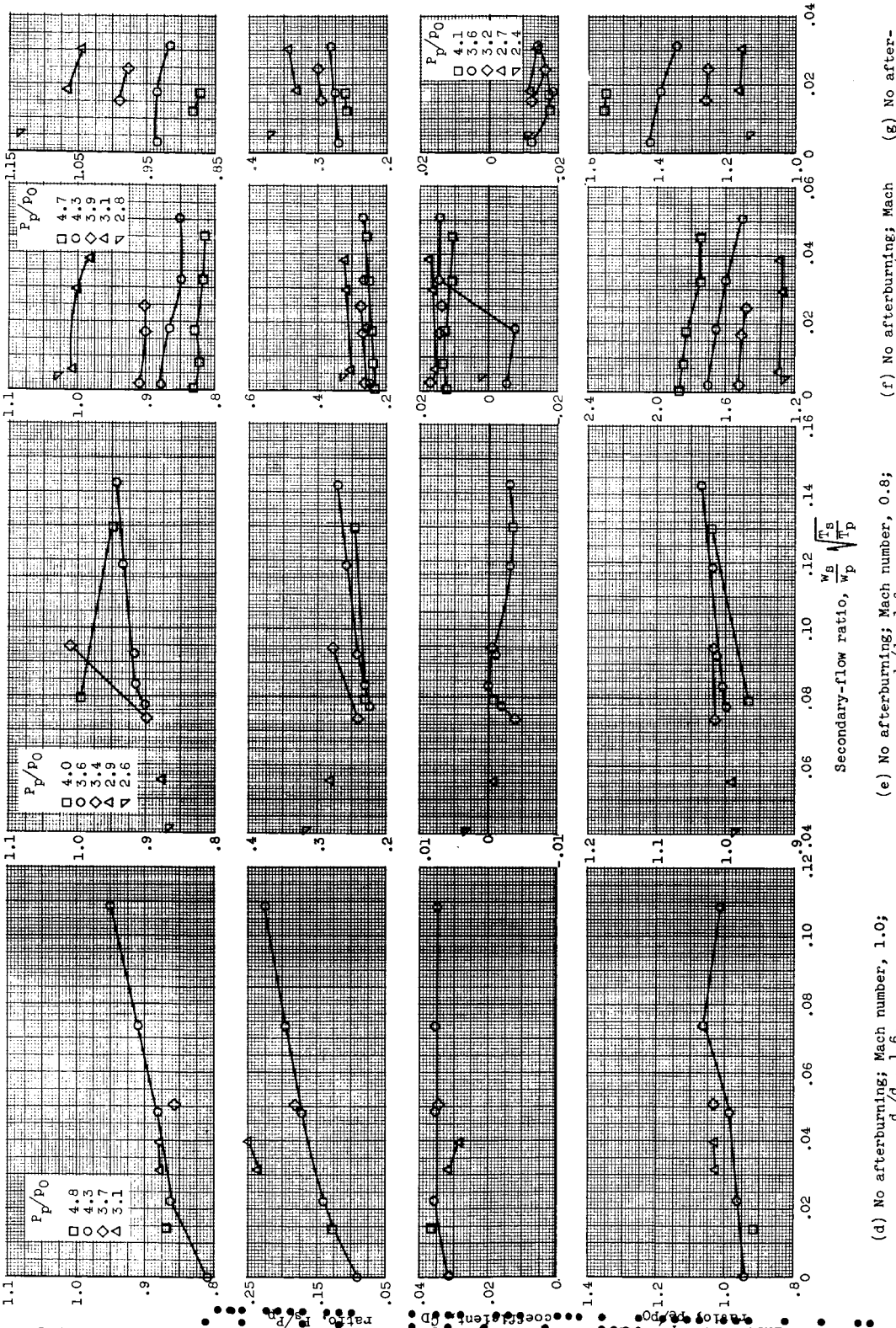

(d) No afterburning; Mach number, 1.0; d_e/d_p, 1.6.

(e) No afterburning; Mach number, 0.8; d_e/d_p, 1.6.

(f) No afterburning; Mach number, 1.0; d_e/d_p, 1.15.

(g) No afterburning; Mach number, 0.8; d_e/d_p, 1.15.

Figure 15. - Concluded. Performance of ejector 7.

UNCLASSIFIED

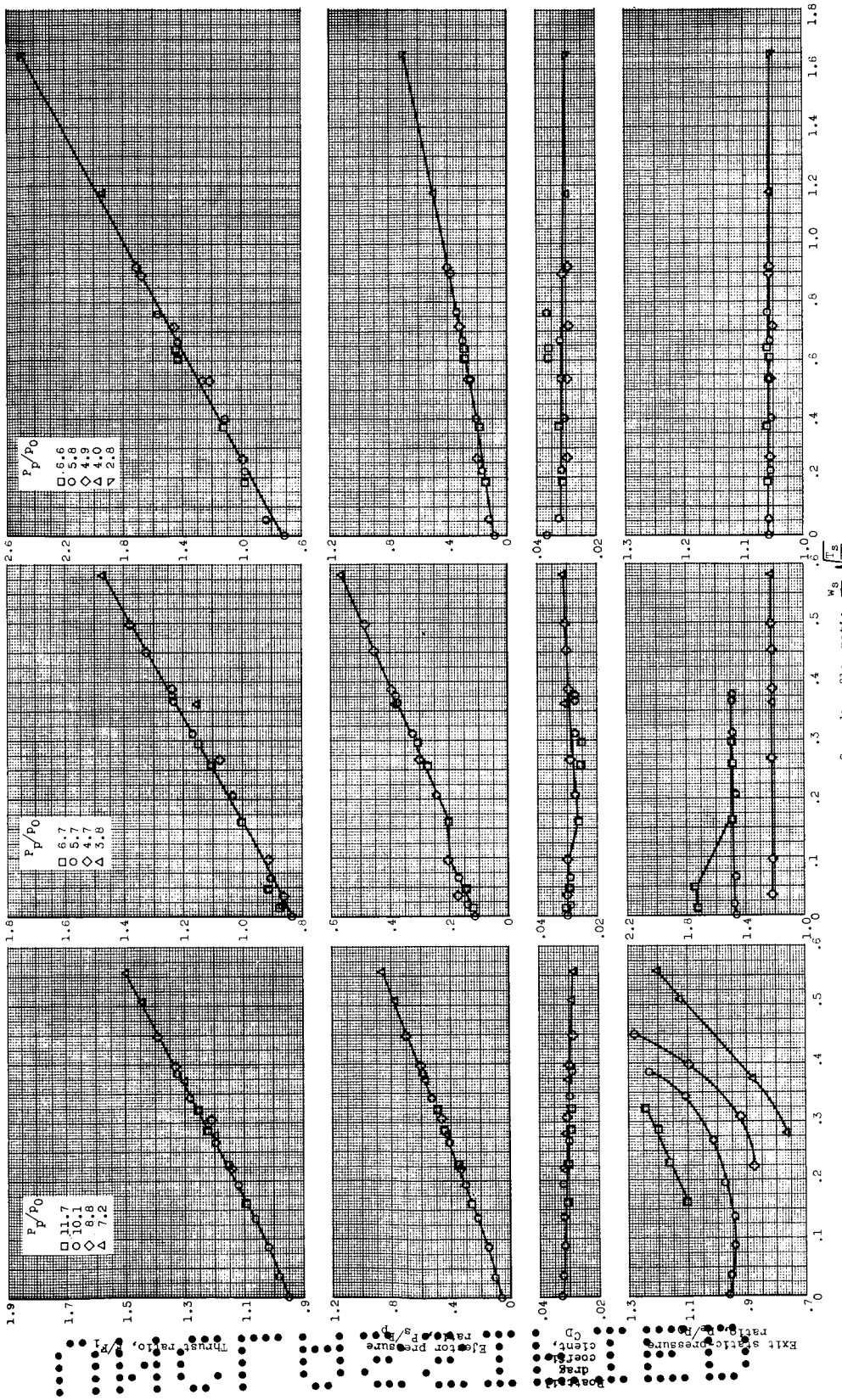

(a) Afterburning; Mach number, 2.0; d_e/d_p, 1.39. (b) Afterburning; Mach number, 1.35; d_e/d_p, 1.15. (c) No afterburning; Mach number, 1.35; d_e/d_p, 1.53.

Figure 16. - Performance of ejector 8 with base flow.

CONFIDENTIAL

UNCLASSIFIED

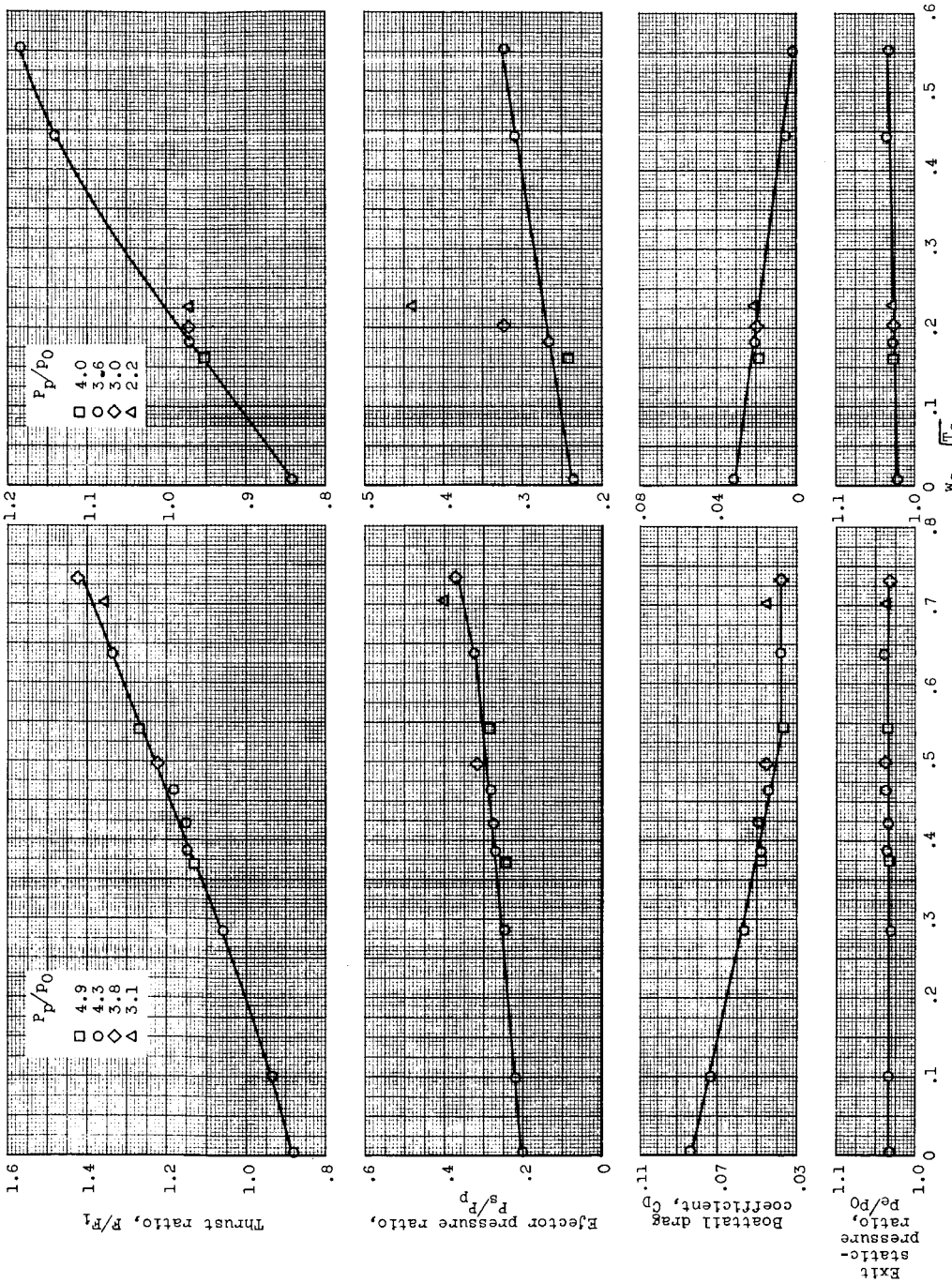

(d) No afterburning; Mach number, 1.0; d_e/d_p, 1.53.

(e) No afterburning; Mach number, 0.8; d_e/d_p, 1.53.

Figure 16. - Concluded. Performance of ejector 8 with base flow.

UNCLASSIFIED

UNCLASSIFIED

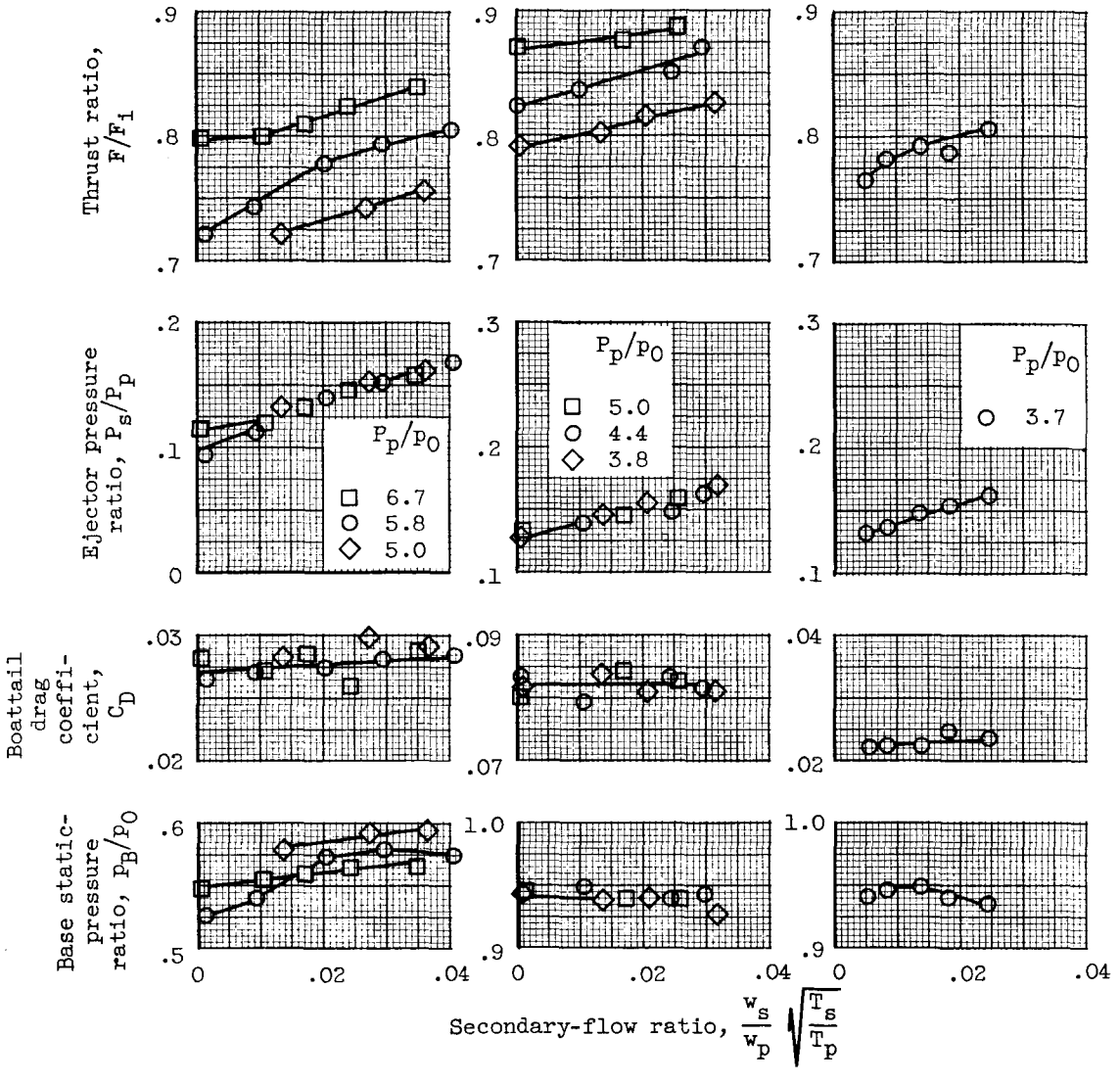

(a) No afterburning; Mach number, 1.35; d_e/d_p, 1.53.

(b) No afterburning; Mach number, 1.0; d_e/d_p, 1.53.

(c) No afterburning; Mach number, 0.8; d_e/d_p, 1.53.

Figure 17. - Performance of ejector 8 without base flow.

UNCLASSIFIED

UNCLASSIFIED

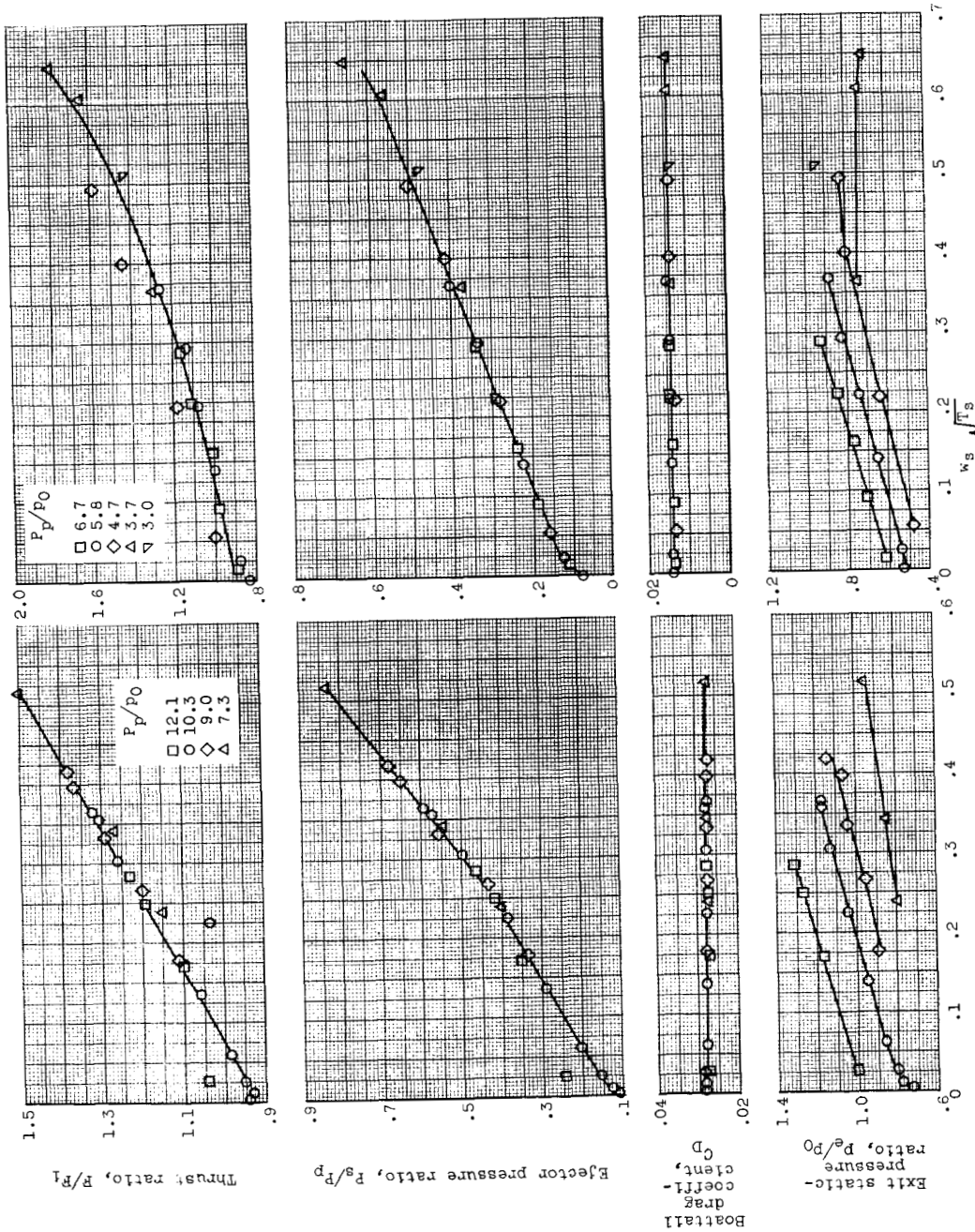

(a) Afterburning; Mach number, 2.0; d_s/d_p, 1.3. (b) Afterburning; Mach number, 1.35; d_s/d_p, 1.45.

Figure 18. - Performance of ejector 9.

UNCLASSIFIED

UNCLASSIFIED

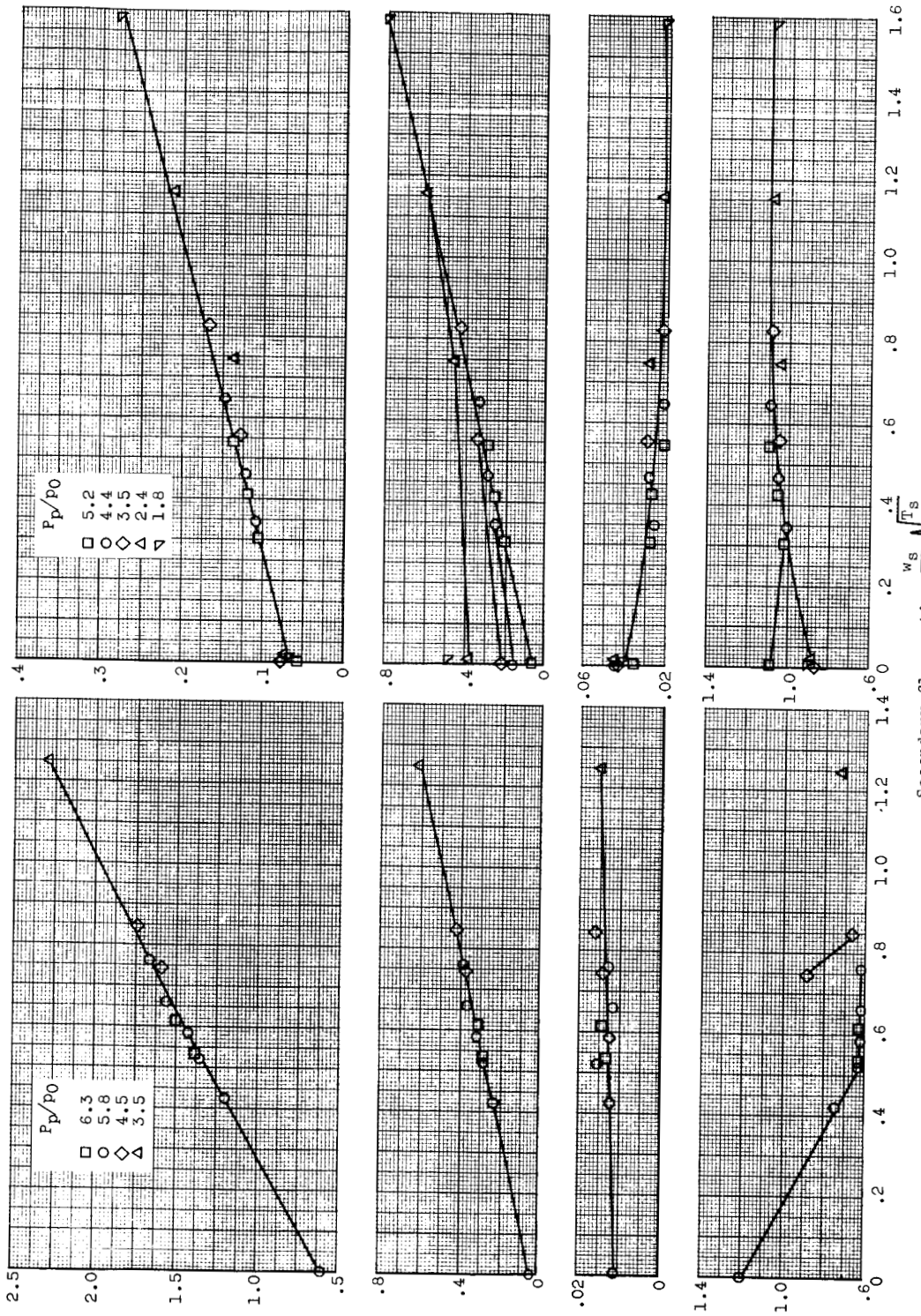

(c) No afterburning; Mach number, 1.35; d_s/d_p, 1.94. (d) No afterburning; Mach number, 1.0; d_s/d_p, 2.14.

Figure 18. - Concluded. Performance of ejector 9.

UNCLASSIFIED

CONFIDENTIAL

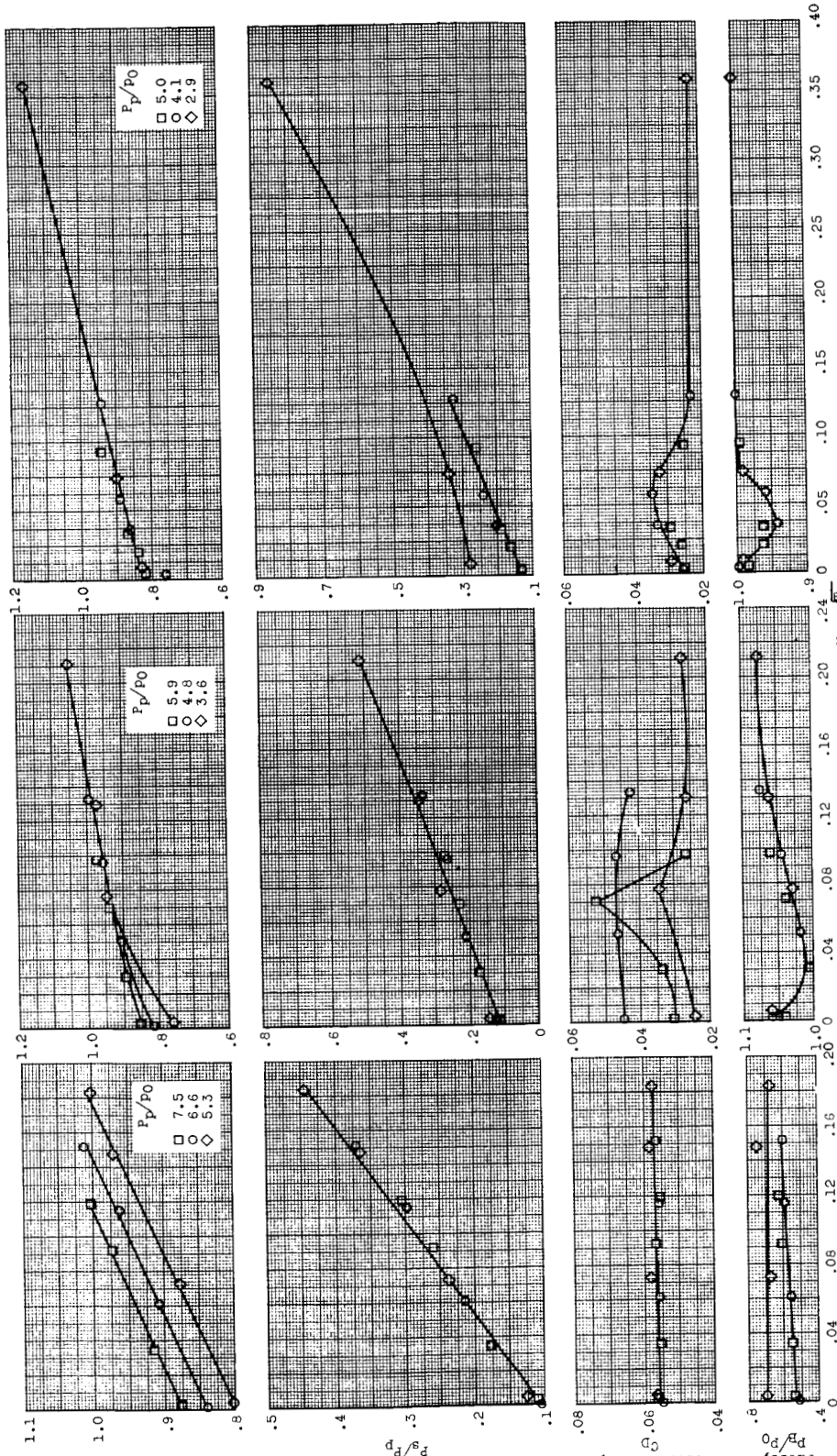

(a) Mach number, 1.35.

(b) Mach number, 1.0.

(c) Mach number, 0.8.

Figure 19. - Performance of ejector 10.

CONFIDENTIAL

UNCLASSIFIED

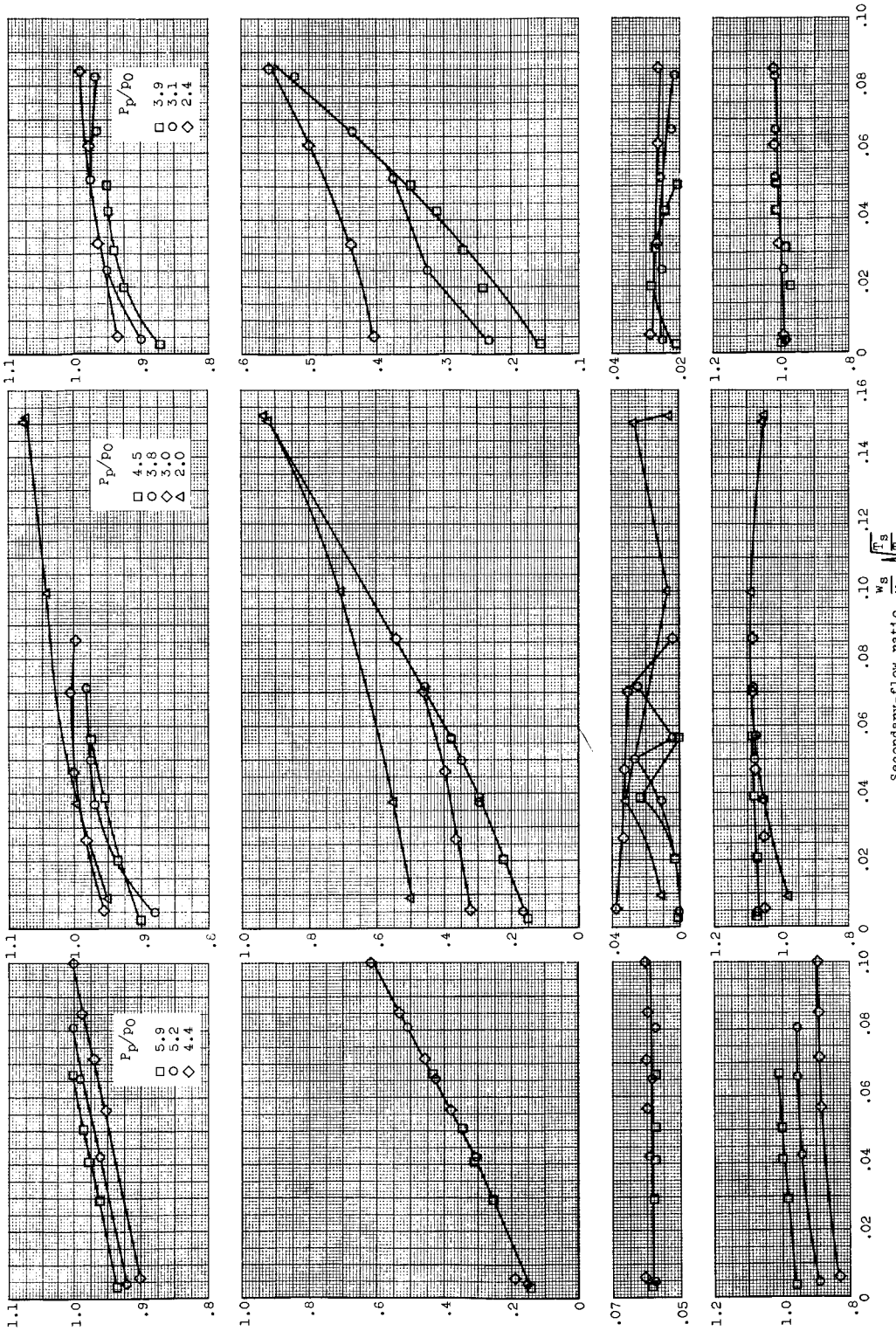

(a) Mach number, 1.35. (b) Mach number, 1.0. (c) Mach number, 0.8.

Figure 20. - Performance of ejector 11.

CONFIDENTIAL

UNCLASSIFIED

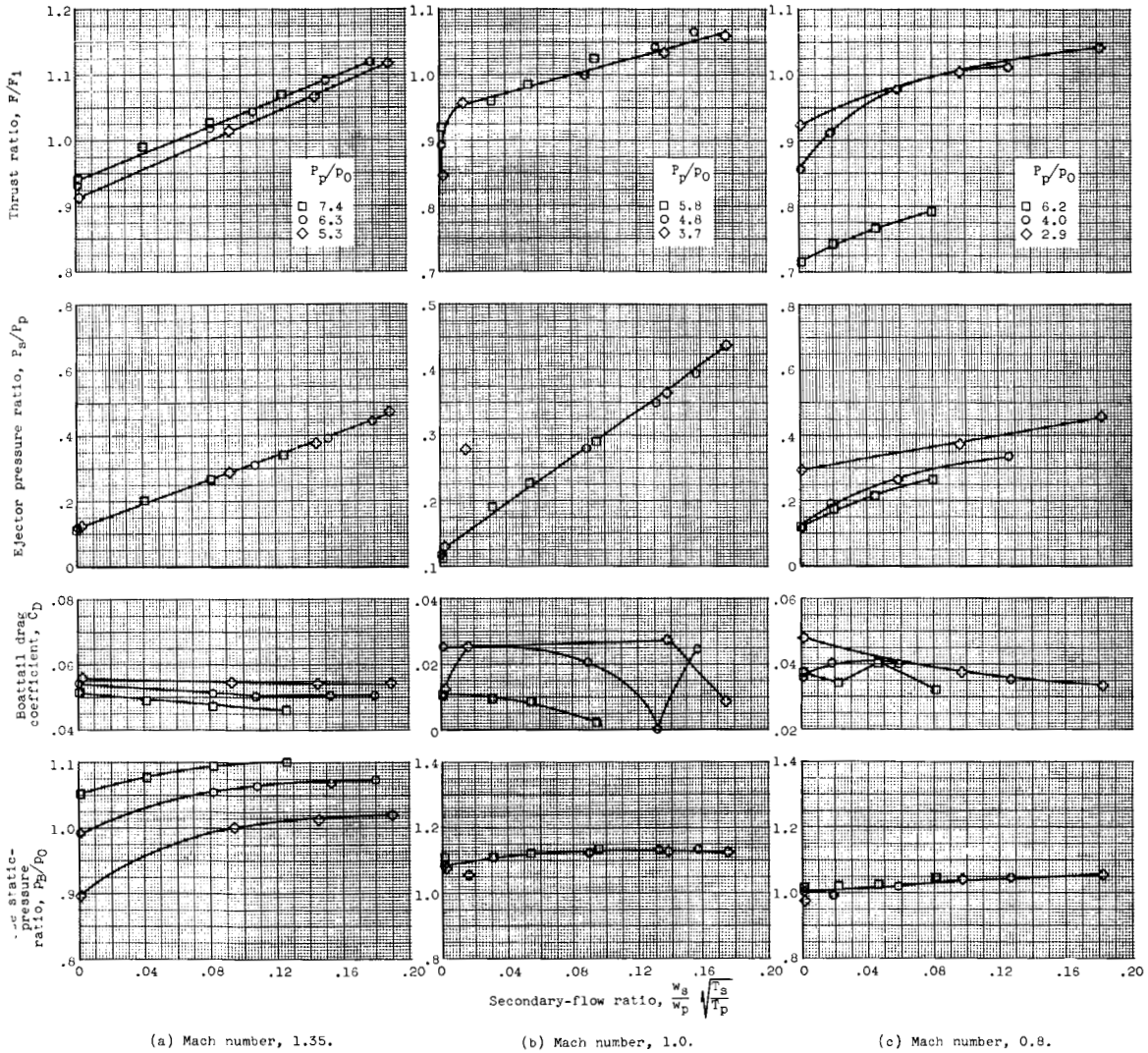

(a) Mach number, 1.35. (b) Mach number, 1.0. (c) Mach number, 0.8.

Figure 21. - Performance of ejector 12.

UNCLASSIFIED

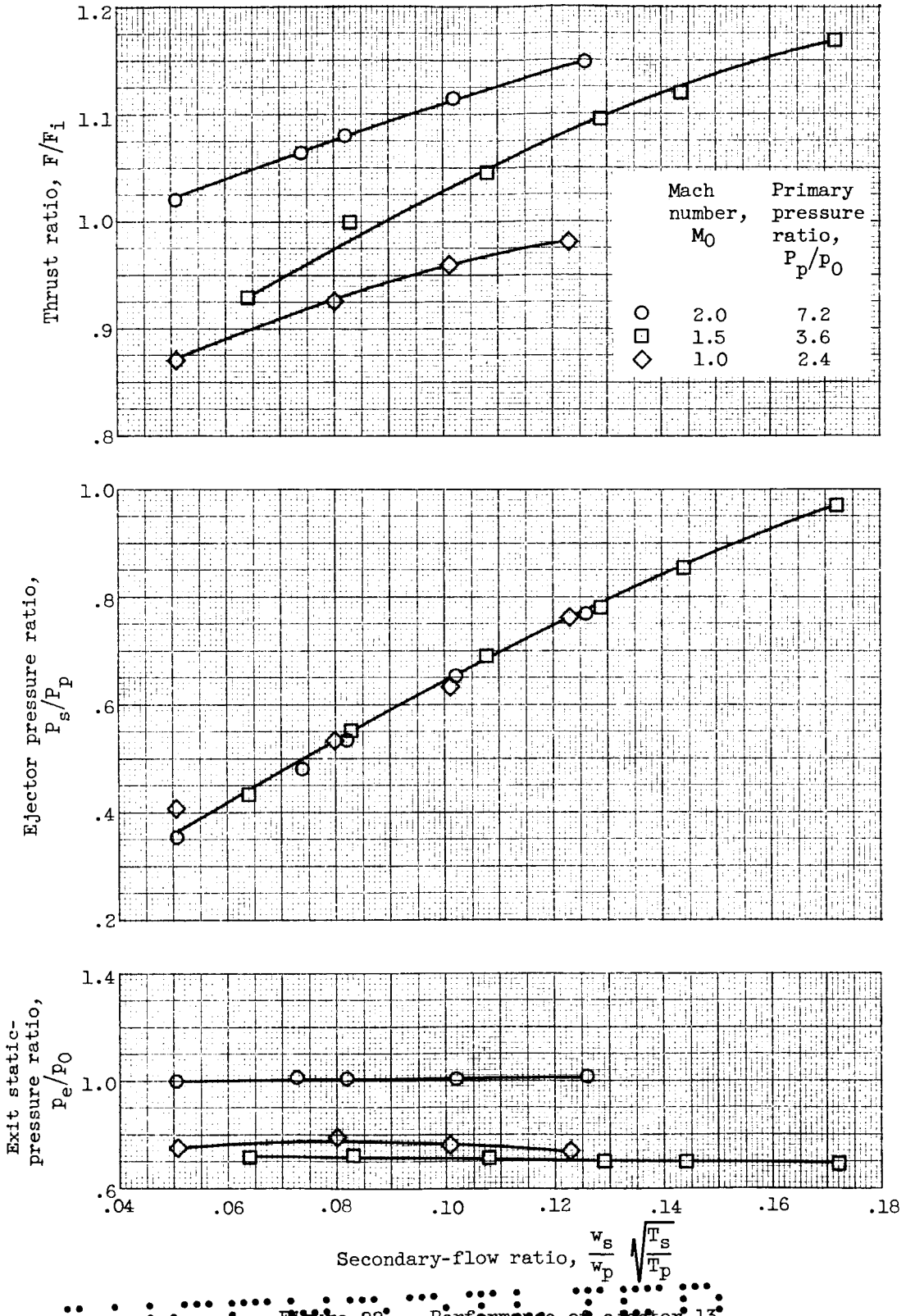

Figure 22. - Performance of ejector 13.

UNCLASSIFIED

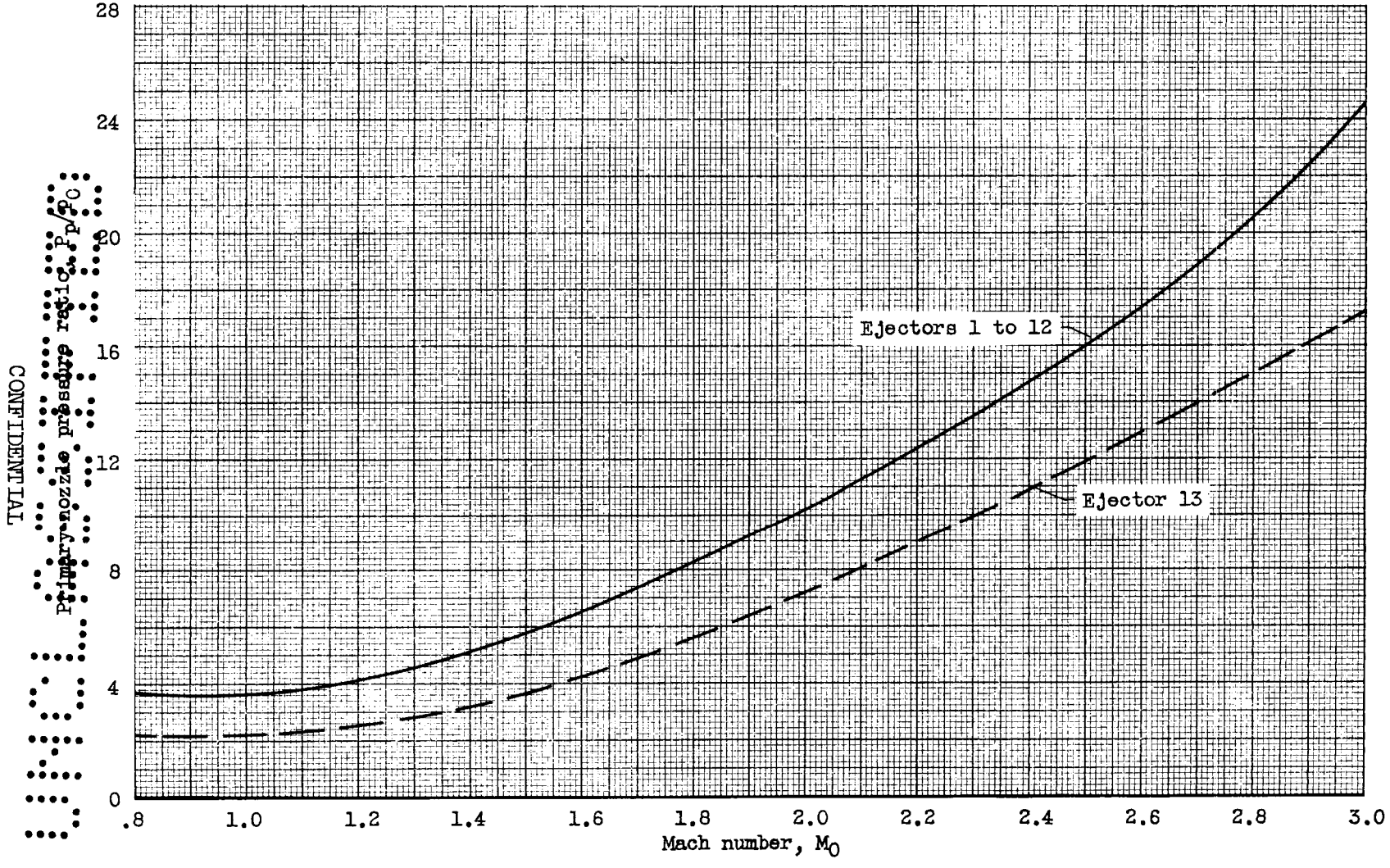

Figure 23. - Schedule of primary-nozzle pressure ratio.

CONFIDENTIAL

UNCLASSIFIED

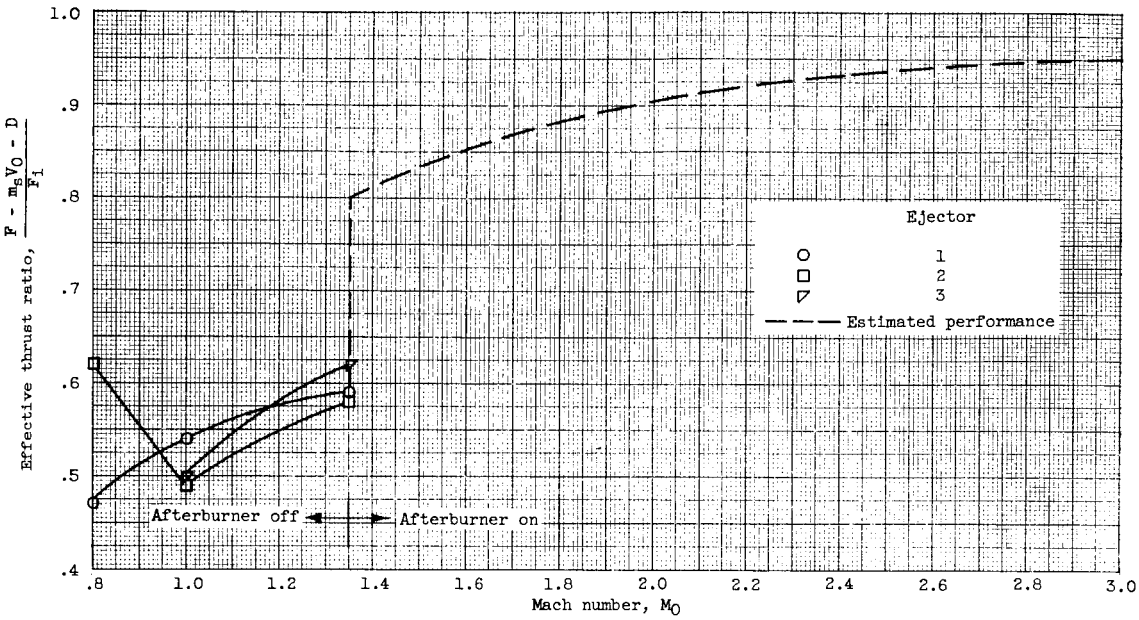

Figure 24. - Effect of flight Mach number on fixed ejector performance. Secondary-flow ratio, 0.02.

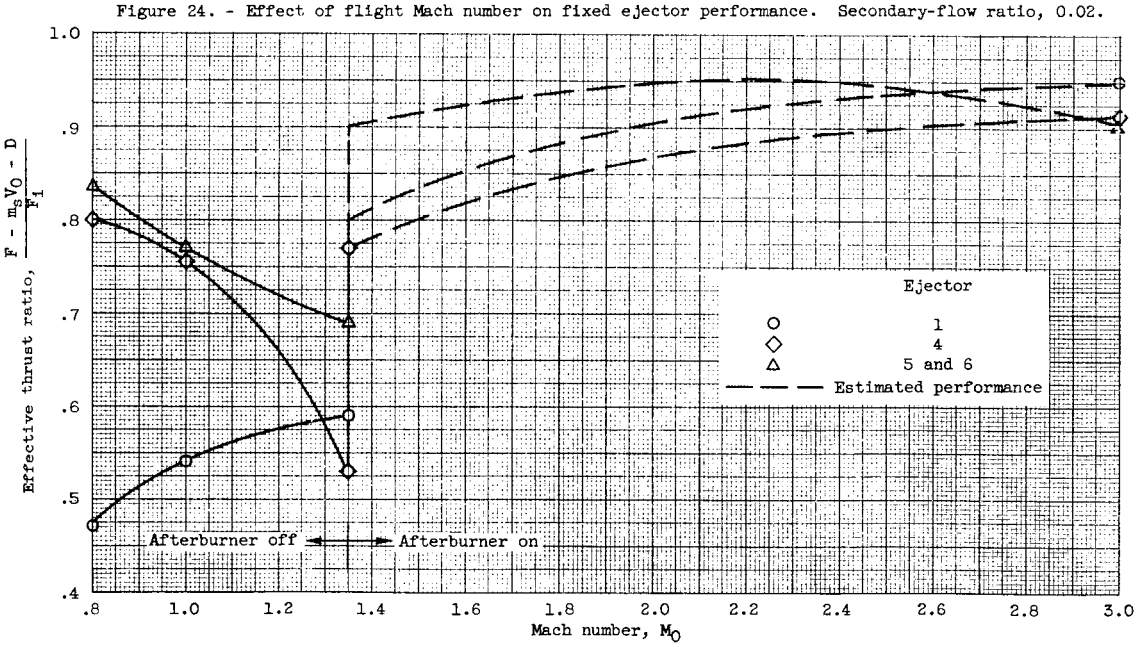

Figure 25. - Effect of design compromises with fixed ejectors. Secondary-flow ratio, 0.02.

UNCLASSIFIED

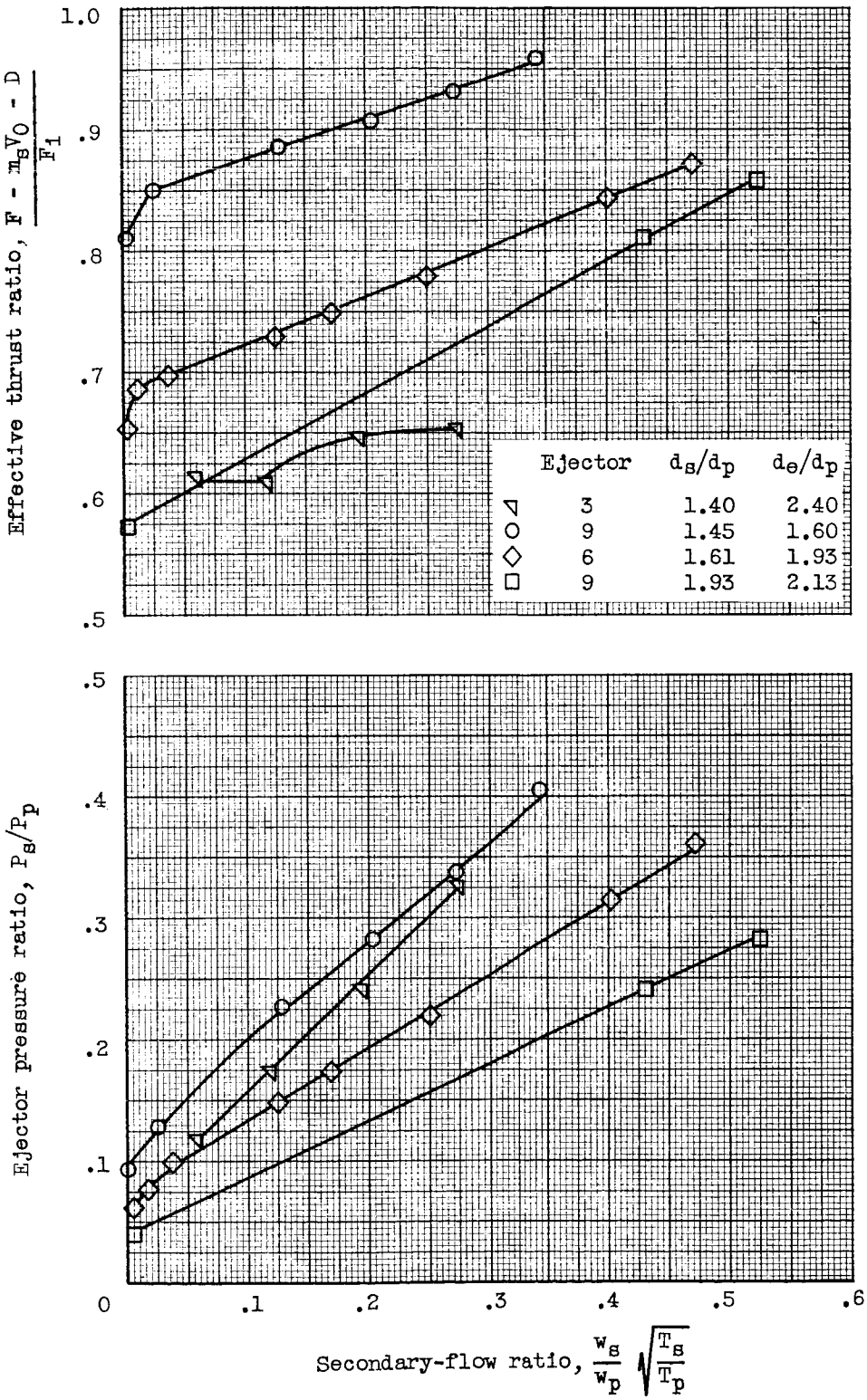

Figure 26. - Effect of secondary flow on fixed ejector performance at Mach 1.35.

UNCLASSIFIED

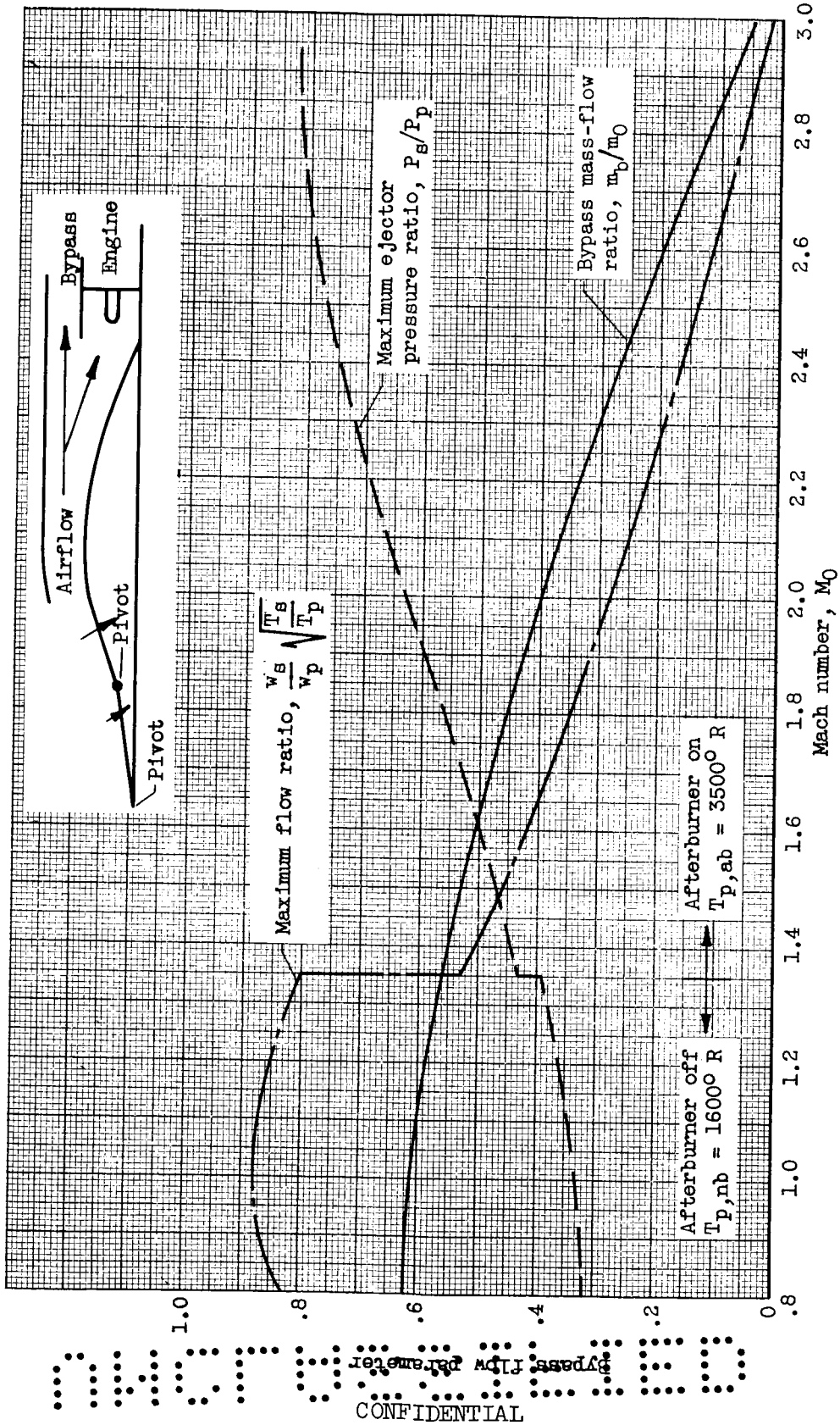

Figure 27. - Schedule of inlet bypass air available for ejector.

UNCLASSIFIED

Figure 28. - Effect of secondary flow on performance of fixed ejector 6.

UNCLASSIFIED

Figure 29. - Effect of spoilers and air injection on performance of fixed ejector 1.

CONFIDENTIAL

UNCLASSIFIED

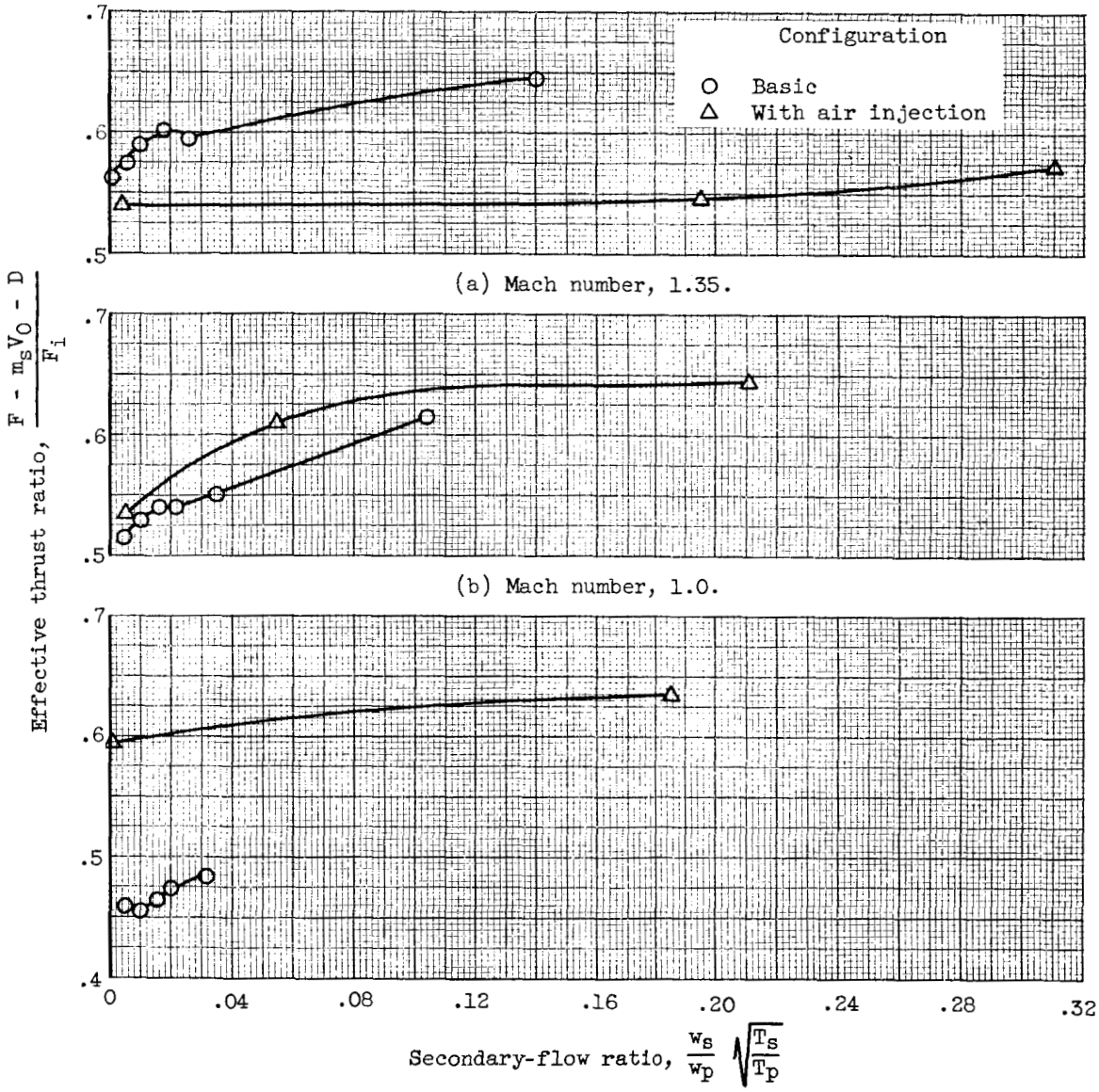

(a) Mach number, 1.35.

(b) Mach number, 1.0.

(c) Mach number, 0.8.

Figure 30. - Air injection compared with high secondary flow with ejector 1 and no afterburning.

UNCLASSIFIED

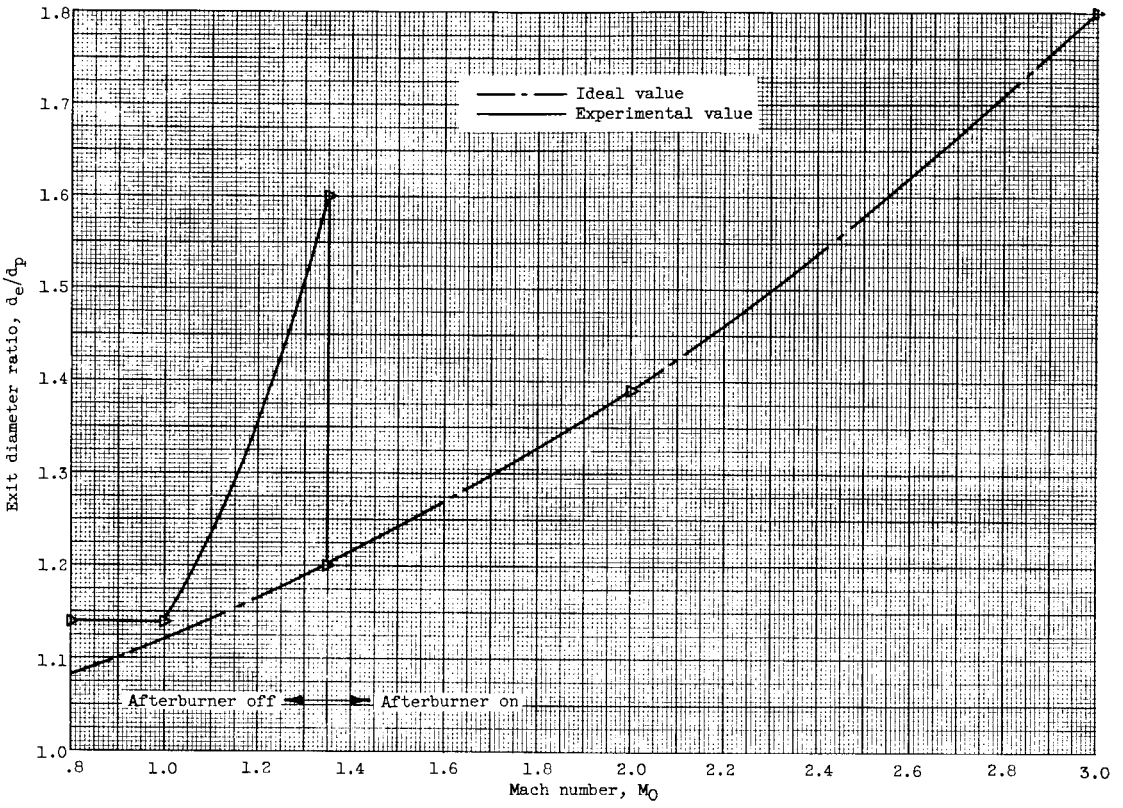

Figure 31. - Expansion-ratio schedule of ejector 7.

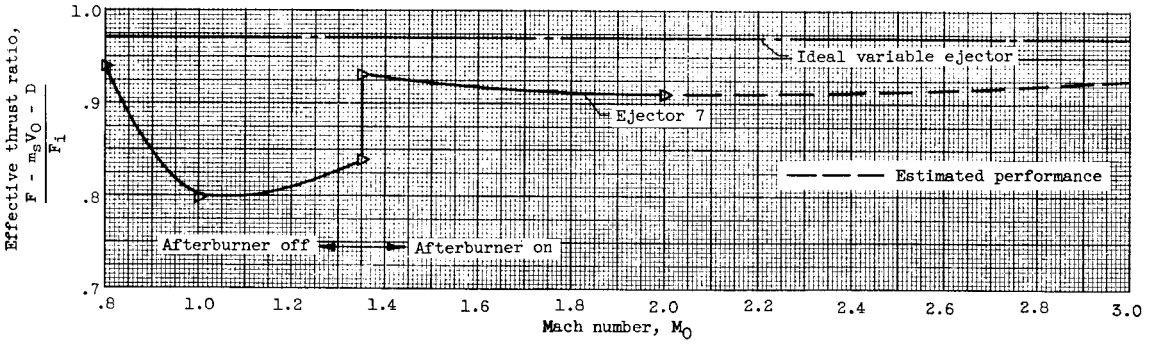

Figure 32. - Effect of design compromises of variable-geometry ejector 7. Secondary-flow ratio, 0.02.

UNCLASSIFIED

CONFIDENTIAL

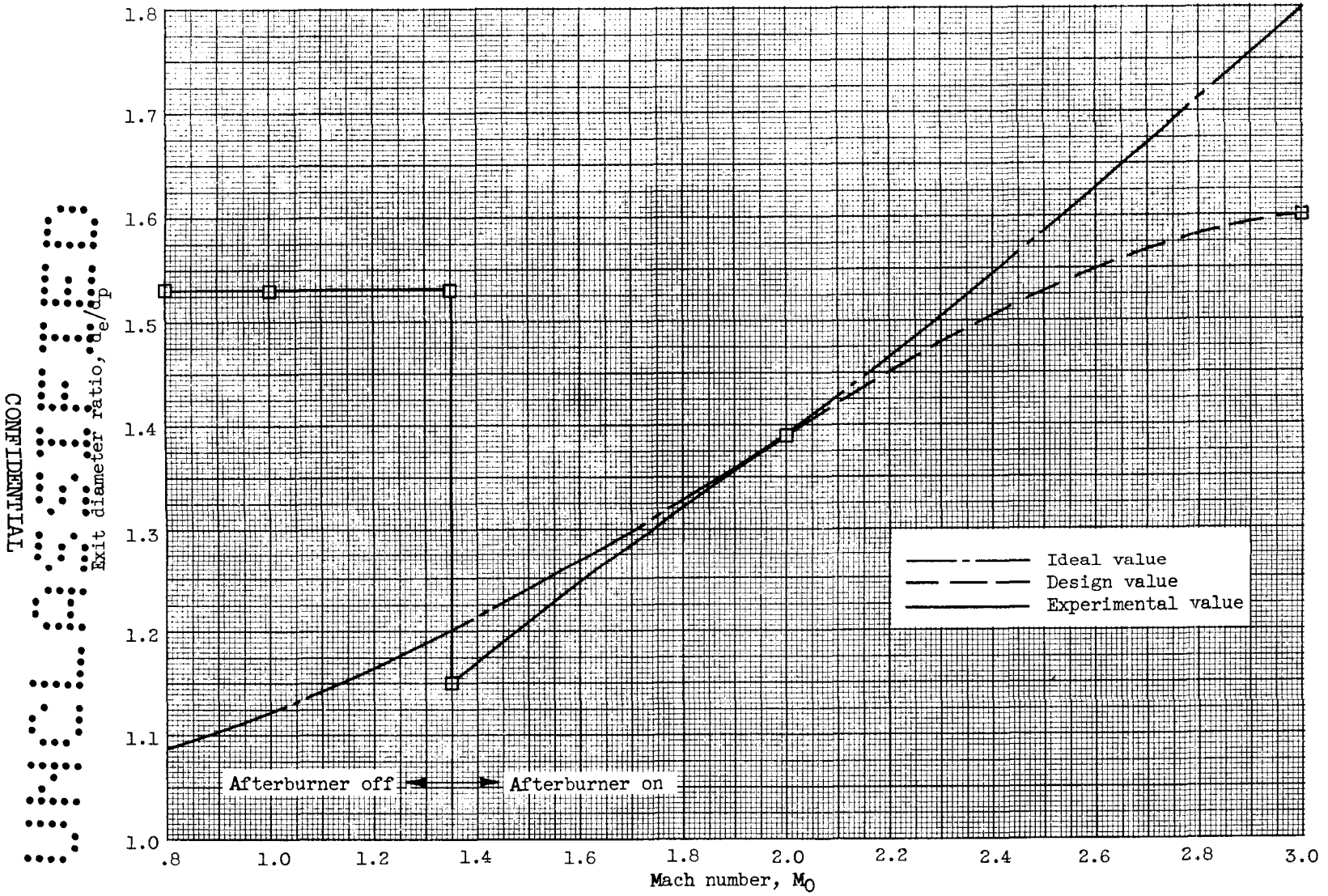

Figure 33. - Expansion-ratio schedule of ejector 8.

UNCLASSIFIED

Figure 34. - Performance of variable-geometry ejector 8.

UNCLASSIFIED

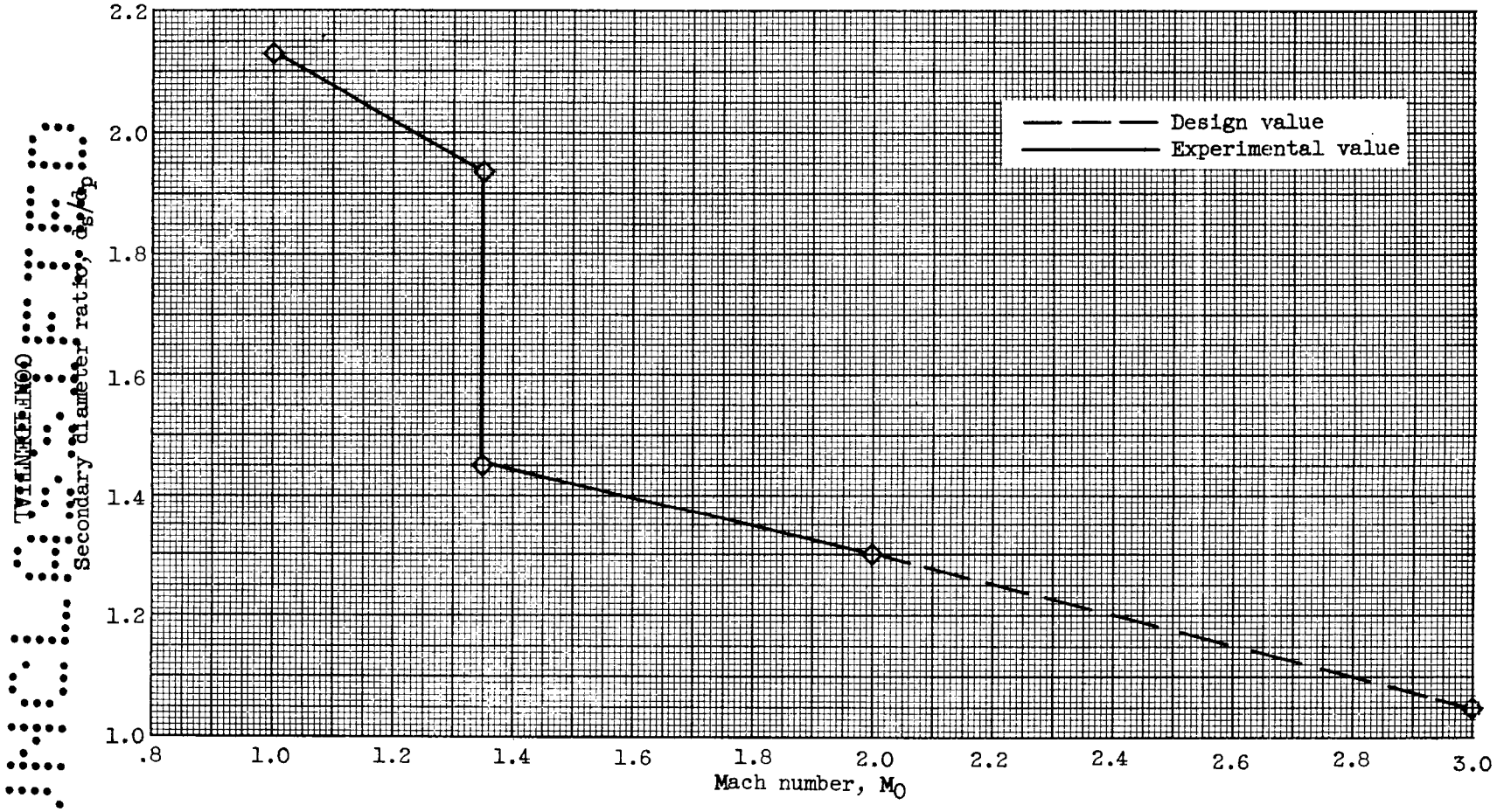

Figure 35. - Secondary-diameter-ratio schedule of ejector 9.

UNCLASSIFIED

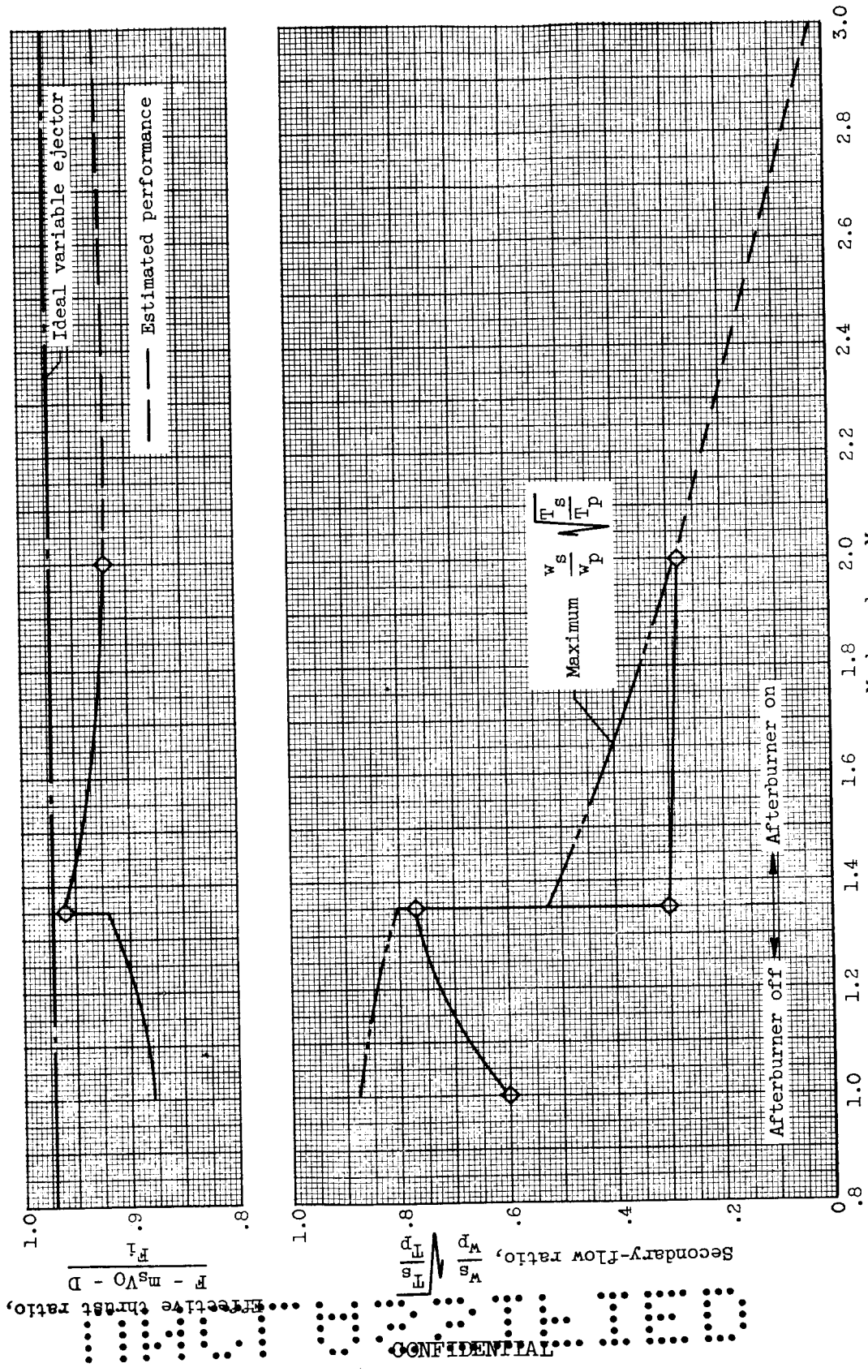

Figure 36. - Performance of variable-geometry ejector 9.

CONFIDENTIAL

UNCLASSIFIED

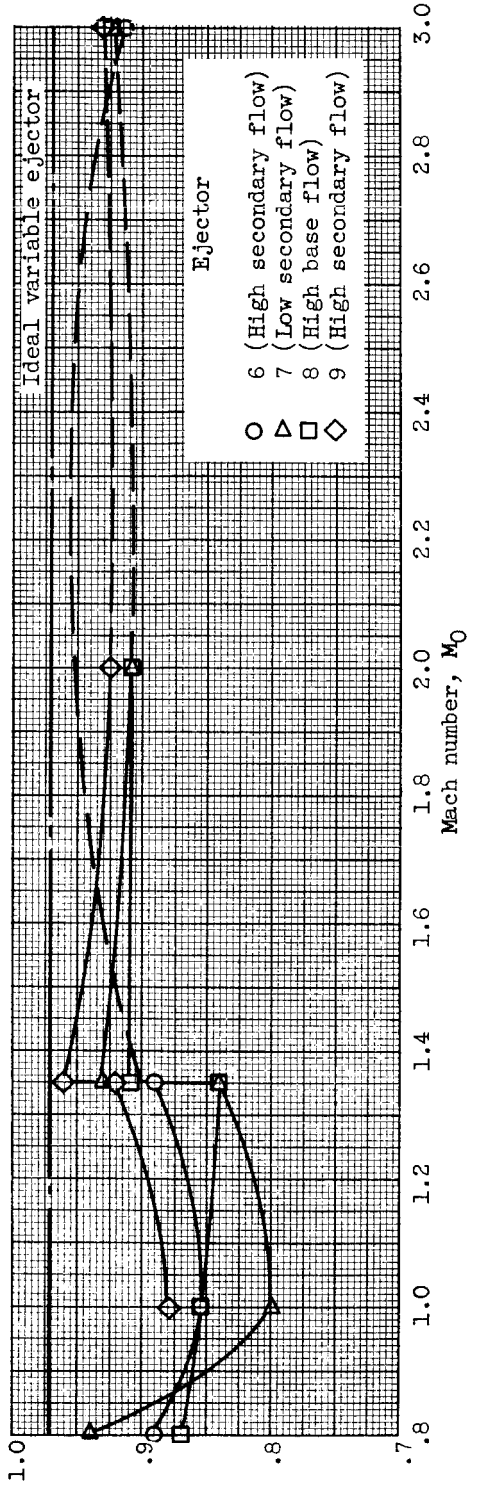

Figure 37. - Summary of performance of best ejector types.

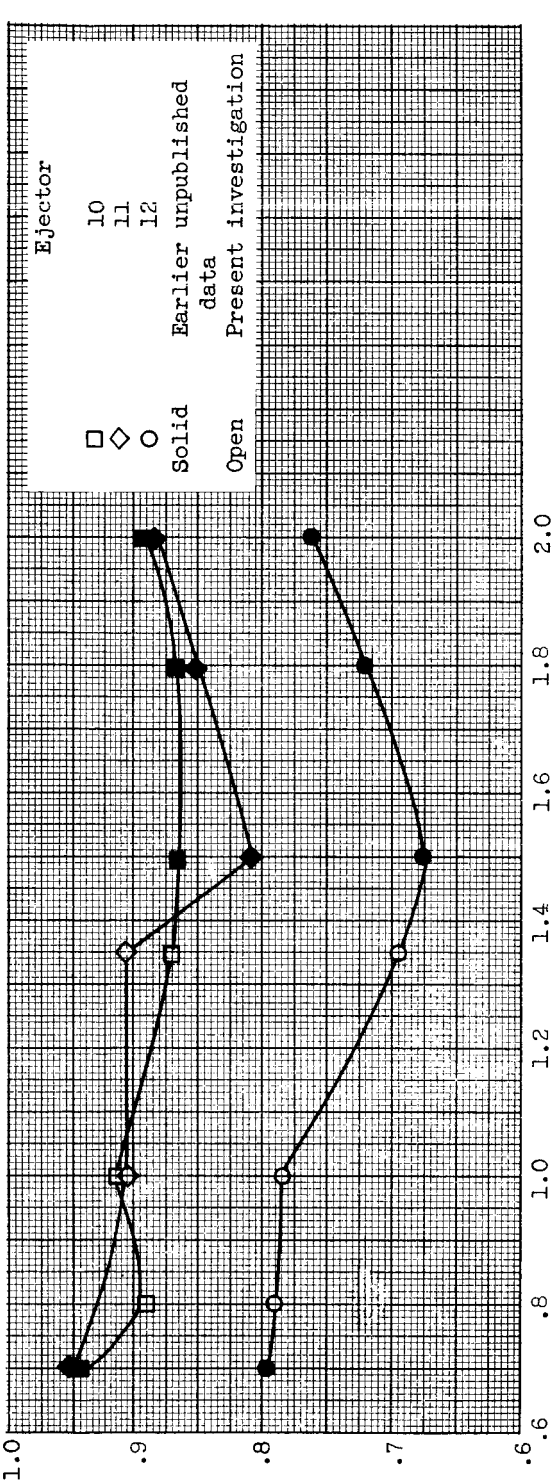

Figure 38. - Effect of Mach number on performance of fixed ejectors 10 to 12. Secondary-flow ratio, 0.02.

CONFIDENTIAL

UNCLASSIFIED

Figure 39. - Effect of secondary flow on performance of fixed ejectors 10 to 12 at Mach number 1.0.

Figure 40. - Effect of secondary flow on performance of ejector 13.

UNCLASSIFIED

ERRATA

NACA RESEARCH MEMORANDUM E58G10a

By Milton A. Beheim

September 1958

Page 43: The title of figure 19 should be "Performance of ejector 12."

Page 44: The title of figure 20 should be "Performance of ejector 10."

Page 45: The title of figure 21 should be "Performance of ejector 11."

Page 60, figure 40: The data symbols ○ and ◇ should be interchanged so that ◇ and ○ represent Mach numbers of 2.0 and 1.0, respectively.

5099

NASA - Langley

Issued July 30, 1959

UNCLASSIFIED

UNCLASSIFIED

UNCLASSIFIED
CONFIDENTIAL

UNCLASSIFIED
CONFIDENTIAL